



(347) – (379)

العدد الرابع عشر

تأثير الدوران وهول على الحركة التمعجية مع تسخين الجول لسائل Powell-Eyring في قناة
غير متناظرة مستدقة مائلة

هناء عبد الحسين ، احمد مولود عبد الهادي

جامعة واسط / كلية التربية الأساسية ، جامعة بغداد / كلية العلوم

ahm6161@yahoo.com ، hshatty@uowasit.edu.iq

المستخلص :

في هذه الدراسة، ناقشنا تأثير الدوران على النقل التمعجي لسائل باويل-إيرنك في قناة مائلة ومدببة وغير متناظرة. تشمل الاعتبارات تأثير هول والانزلاق الحراري وظروف انزلاق السرعة وتسخين الجول. من خلال الأخذ في الاعتبار التقريبات المنخفضة لعدد رينولدز وطول الموجة الطويل، يتم نمذجة المعادلات الحاكمة لمعادلات الاستمرارية والحركة والطاقة ومن ثم يتم تبسيطها. وقد لوحظ أن تأثير الدوران على السرعة ودالة الجريان ودرجة الحرارة يزداد بينما يتناقص معامل انتقال الحرارة مع زيادته. التأثير المعاكس بين رقم هارتمان ومتغير هول واضح في الدراسة. الطريقة المستخدمة لتحديد حل أنظمة المعادلات هي تقنية الاضطراب، والتي تمت دراستها باستخدام برنامج "MATHEMATICA".

الكلمات المفتاحية : سائل باويل-إيرنك ، نقل الحرارة ، تأثير هول.

Effect of Rotation and Hall on Peristaltic Movement with Joule Heating for Powell-Eyring Fluid in an Inclined Tapered Asymmetrical Channel

Hanaa Abdulhussein ، Ahmed M. Abdulhadi

Wasit University / College of Basic Education , University of Baghdad /College of Science

hshatty@uowasit.edu.iq ، ahm6161@yahoo.com

**Abstract :**

In this study, we discussed the impact of rotation on the peristaltic transport of Powell-Eyring fluid in an inclined, tapered, asymmetrical channel. Considerations include the Hall effect, thermal slip, velocity slip conditions and joule heating. By keeping in mind the low Reynolds number approximations and long wavelength, the governing equations for the equations of continuity, motion, and energy are modeled and then made simpler. It has been noted that the effect of rotation on the axial velocity, stream function and temperature increases while the heat transfer coefficient decreases with its increase. The opposite effect between the Hartmann number and the Hall parameter is evident in the study. The method used to locate the solution to systems of equations is the perturbation technique, which is studied using the MATHEMATICA software.

Keywords: Powell-Eyring fluid, heat transfer, Hall effect .

1. Introduction

The peristaltic movement has garnered substantial interest in recent years due to its applications in engineering, physiological, and biological structures. The peristalsis as a whole refers to consecutive longitudinal and cyclic contractions generated by sinusoidal stimulation waves that go through the channel and propagate, enclosing the fluid. Specifically, this mechanism is the foundation of numerous muscle tubes, including the digestive system, fallopian tube, bile duct, ureter, esophagus tube, etc. Additionally, it plays a crucial role in several industrial applications, including the transfer of sanitary fluid, blood pumps in heart-lung machines, and the transmission of corrosive fluids (Ramesh & Devakar, 2017) and (Murad & Abdulhadi, 2020).

Non-Newtonian fluids alter their viscosity or flow behavior when subjected to stress. However, not all non-Newtonian fluids exhibit the same response; some become more solid while others become more fluid. Some



non-Newtonian fluids react to the amplitude of the applied stress, whereas others react to the duration of the stress. The Powell-Eyring model is mathematically more complex but deserves distinct advantages over the non-Newtonian model because of its fluid models. Studies have been done on the peristaltic flow of Powell-Eyring fluid with a long wavelength, a low Reynolds number, and different flow conditions (Hina, 2016), (Abdulhussein & Abdalhadi, 2022) and (Ali & Abdalhadi, 2018).

In the presence of a strong magnetic field, the investigation of Hall's effect becomes crucial. These effects are particularly valuable in a range of sectors, including power generators, magnetometers for detecting magnetic fields, transformers, Hall current sensors, fuel level indicators for automobiles, spacecraft propulsion, and magnetic status monitoring in DC electric motors. (Hayat et al. 2017) studied the effect of Hall on the peristaltic motion of a Powell-Eyring fluid in an inclined symmetric canal. (Hasen et al. 2022) analyzed the effect of Hall current and Joule heating on the peristaltic pumps of the Fene-P model. (NABIL & DOAA, 2020), (Asfour, 2020), and (Hassen & Ali, 2021) reported different fluid Hall current effects. In porous media with non-symmetric canals, rotating waveform motion in two-dimensional channels of non-Newtonian fluid was explored by (Alshareef, 2020). Discuss the influence of rotation on the mixed convection heat transfer analysis by (Mohaisen & Abdalhadi, 2021) for viscoplastic fluid peristaltic transport.

This study aims to investigate the effects of the rotation of heat transfer on the peristaltic transport of a Powell-Eyring in an inclined, asymmetrically tapered channel. We will look at the Hall effect, velocity slip, thermal slip conditions, and joule heating. A regular perturbation technique may be used to solve a set of equations under long wavelength and low Reynolds number assumptions.



an asymmetry with out-of-phase waves, whereas $\phi_1 = \pi$ relates to waves that are in phase, ($\bar{M} \ll 1$) \bar{M} is a non-uniform parameter. Furthermore, a^*, b^*, d_1, d_2 and ϕ_1 satisfy the following condition;

$$a^{*2} + b^{*2} + 2a^*b^* \cos\phi_1 \leq (d_1 + d_2)^2.$$

The fluid's Cauchy stress tensor (τ) under the Powell-Eyring model (Ali & Abdulhadi, 2018):

$$\tau = -PI + \bar{S}$$

(3)

$$\bar{S} = \left[\mu + \frac{1}{\beta \dot{\gamma}} \sinh^{-1} \left(\frac{\dot{\gamma}}{c_1} \right) \right] B_1$$

(4)

$$\dot{\gamma} = \sqrt{\frac{1}{2} \text{tra}(B_1^2)}$$

(5)

$$B_1$$

$$= \nabla \vec{V} + (\nabla \vec{V})^T$$

(6)

Where $\vec{V} = (\tilde{U}, \tilde{V}, 0)$ is the velocity vector, $-PI$ is the spherical part of stress due to constraining of compressibility, \bar{S}_{ij} ($i, j = \bar{X}, \bar{Y}$) is the components of extra stress tensor, μ is the dynamic viscosity and β, c_1 the material parameters of Powell-Eyring fluid. The term \sinh^{-1} can be approximated as

$$\sinh^{-1} \left(\frac{\dot{\gamma}}{c_1} \right) = \frac{\dot{\gamma}}{c_1} - \frac{\dot{\gamma}^3}{6c_1^3}, \quad \left| \frac{\dot{\gamma}^5}{c_1^5} \right| \ll 1 \quad (7)$$

The generalized Ohms law with Hall effects is

$$\vec{J} = \sigma \left[\vec{V} \times \vec{B} - \frac{1}{en} (\vec{J} \times \vec{B}) \right] \quad (8)$$

$$(\vec{J} \times \vec{B}) = \left(\frac{-\sigma B^2 (\tilde{U} - m\tilde{V})}{1+m^2} i - \frac{-\sigma B^2 (\tilde{V} + m\tilde{U})}{1+m^2} j \right) \quad (9)$$



In which \vec{j} characterize the current density vector, n the number density of electron, e the electric charge, B_0 the magnetic field strength and $\left(m = \frac{\sigma B_0}{en}\right)$ the Hall parameter.

The governing equations, continuity, momentum, and energy, in two dimensions are:

$$\frac{\partial \tilde{U}}{\partial \tilde{x}} + \frac{\partial \tilde{V}}{\partial \tilde{y}} = 0 \quad (10)$$

$$\rho \left(\frac{\partial \tilde{U}}{\partial \tilde{t}} + \tilde{U} \frac{\partial \tilde{U}}{\partial \tilde{x}} + \tilde{V} \frac{\partial \tilde{U}}{\partial \tilde{y}} \right) - \rho \Omega \left(\Omega \tilde{U} + 2 \frac{\partial \tilde{V}}{\partial \tilde{t}} \right) = - \frac{\partial \tilde{P}}{\partial \tilde{x}} + \frac{\partial \bar{S}_{XX}}{\partial \tilde{x}} + \frac{\partial \bar{S}_{XY}}{\partial \tilde{y}} - \frac{\sigma B_0^2 (\tilde{U} - m \tilde{V})}{1+m^2} + \rho g \sin \alpha \quad (11)$$

$$\rho \left(\frac{\partial \tilde{V}}{\partial \tilde{t}} + \tilde{U} \frac{\partial \tilde{V}}{\partial \tilde{x}} + \tilde{V} \frac{\partial \tilde{V}}{\partial \tilde{y}} \right) - \rho \Omega \left(\Omega \tilde{V} - 2 \frac{\partial \tilde{U}}{\partial \tilde{t}} \right) = - \frac{\partial \tilde{P}}{\partial \tilde{y}} + \frac{\partial \bar{S}_{YX}}{\partial \tilde{x}} + \frac{\partial \bar{S}_{YY}}{\partial \tilde{y}} - \frac{\sigma B_0^2 (\tilde{V} + m \tilde{U})}{1+m^2} - \rho g \cos \alpha \quad (12)$$

$$\rho C_p \left(\frac{\partial T}{\partial \tilde{t}} + \tilde{U} \frac{\partial T}{\partial \tilde{x}} + \tilde{V} \frac{\partial T}{\partial \tilde{y}} \right) = \tilde{K} \left(\frac{\partial^2 T}{\partial \tilde{x}^2} + \frac{\partial^2 T}{\partial \tilde{y}^2} \right) + (\bar{S}_{YY} - \bar{S}_{XX}) \frac{\partial \tilde{V}}{\partial \tilde{y}} + \bar{S}_{XY} \left(\frac{\partial \tilde{U}}{\partial \tilde{y}} + \frac{\partial \tilde{V}}{\partial \tilde{x}} \right) + \frac{\sigma B_0^2 (\tilde{U}^2 + \tilde{V}^2)}{1+m^2} \quad (13)$$

Here Ω is rotation, \tilde{P} is the fluid pressure, ρ is density of fluid . Additionally, the channel inclined at angle α . There is an applied strong magnetic field of $(0,0,B_0)$. The thermal contributions of Hall and Joule are kept. T is the temperature, g is the acceleration by gravity, C_p is the specific heat at constant pressure. σ is the fluids electrical conductivity, \tilde{K} is the thermal conductivity. The induced electric field is not taken into consideration at all, because assuming a low magnetic Reynolds number.

The stress components are given by the form



$$\bar{S}_{\bar{X}\bar{X}} = 2 \left(\mu + \frac{1}{\beta c_1} \right) \bar{U}_{\bar{X}} - \frac{1}{3\beta c_1^3} \left[2\bar{U}_{\bar{X}}^2 + (\bar{U}_{\bar{Y}} + \bar{V}_{\bar{X}})^2 + 2\bar{V}_{\bar{Y}}^2 \right] \bar{U}_{\bar{X}} \quad (14)$$

$$\begin{aligned} \bar{S}_{\bar{X}\bar{Y}} = & \left(\mu + \frac{1}{\beta c_1} \right) (\bar{V}_{\bar{X}} + \bar{U}_{\bar{Y}}) \\ & - \frac{1}{6\beta c_1^3} \left[2\bar{U}_{\bar{X}}^2 + (\bar{U}_{\bar{Y}} + \bar{V}_{\bar{X}})^2 + 2\bar{V}_{\bar{Y}}^2 \right] (\bar{V}_{\bar{X}} \\ & + \bar{U}_{\bar{Y}}) \end{aligned} \quad (15)$$

$$\bar{S}_{\bar{Y}\bar{Y}} = 2 \left(\mu + \frac{1}{\beta c_1} \right) \bar{V}_{\bar{Y}} - \frac{1}{3\beta c_1^3} \left[2\bar{U}_{\bar{X}}^2 + (\bar{U}_{\bar{Y}} + \bar{V}_{\bar{X}})^2 + 2\bar{V}_{\bar{Y}}^2 \right] \bar{V}_{\bar{Y}} \quad (16)$$

The slip conditions for velocity and temperature at the walls are:

$$\bar{U} \pm \xi^* \bar{S}_{\bar{X}\bar{Y}} = 0 \text{ at } \bar{Y} = \bar{H}_1 \text{ and } \bar{Y} = \bar{H}_2 \quad (17)$$

$$T \pm \beta_1^* \frac{\partial T}{\partial \bar{Y}} = T_0 \text{ at } \bar{Y} = \bar{H}_1 \text{ and } \bar{Y} = \bar{H}_2 \quad (18)$$

Flexible walls are given as

$$\begin{aligned} \left[-\tau \frac{\partial^3}{\partial \bar{X}^3} + m_2 \frac{\partial^3}{\partial \bar{X} \partial \bar{t}^2} + d^0 \frac{\partial^2}{\partial \bar{t} \partial \bar{X}} \right] \bar{Y} = & \frac{\partial \bar{S}_{\bar{X}\bar{X}}}{\partial \bar{X}} + \frac{\partial \bar{S}_{\bar{X}\bar{Y}}}{\partial \bar{Y}} - \frac{\sigma B^2 (\bar{U} - m\bar{V})}{1+m^2} + \rho g \sin \alpha - \\ \rho \left(\frac{\partial \bar{U}}{\partial \bar{t}} + \bar{U} \frac{\partial \bar{U}}{\partial \bar{X}} + \bar{V} \frac{\partial \bar{U}}{\partial \bar{Y}} \right) & \text{ at } \bar{Y} = \bar{H}_1 \text{ and } \bar{Y} = \bar{H}_2 \end{aligned} \quad (19)$$

مجلة العلوم الأساسية
للعلوم التربوية والنفسية وطرائق التدريس للعلوم الأساسية

In the above ξ^* , β_1^* , T_0 , m_2 , τ , d^0 are the velocity slip parameter, thermal slip parameter, the temperature at the upper and lower walls, the mass per unit area, elastic tension and the coefficient of viscous damping respectively.

To reduce the number of additional parameters, we shall define the following non-dimensional quantities:

$$y = \frac{\bar{Y}}{d_1}, x = \frac{\bar{X}}{\lambda}, h1 = \frac{\bar{H}_1}{d_1}, h2 = \frac{\bar{H}_2}{d_1}, \theta = \frac{T - T_0}{T_0}, u = \frac{\bar{U}}{c}, v = \frac{\bar{V}}{\delta c}, p = \frac{d_1^2 \bar{P}}{\lambda \mu c},$$



$$t = \frac{c\bar{t}}{\lambda}, R_e = \frac{c\rho d_1}{\mu}, M = \frac{\bar{M}\lambda}{d_1}, \delta = \frac{d_1}{\lambda}, H = B \cdot d_1 \sqrt{\frac{\sigma}{\mu}}, P_r = \frac{\mu C_p}{K}, F_r = \frac{c^2}{g d_1},$$

$$\xi = \frac{\xi^*}{d_1}, \beta_1 = \frac{\beta_1^*}{d_1}, B_r = P_r \cdot E_c, E_c = \frac{c^2}{T_0 C_p}, a = \frac{a^*}{d_1}, b = \frac{b^*}{d_1}, S_{ij} = \frac{d_1 \bar{S}_{ij}}{\mu c}$$

(20)

$$W_1 = \frac{1}{\mu \beta c_1}, B = \frac{W_1}{6} \left(\frac{c}{c_1 d_1} \right)^2, E_1 = \frac{-\tau d_1^3}{\lambda^3 \mu c}, E_2 = \frac{m_2 c d_1}{\lambda^3 \mu c}, E_3 = \frac{d^{\circ} d_1}{\lambda^2 \mu}$$

Where $\theta, R_e, M, \delta, H, P_r, F_r, B_r, E_c, E_1, E_2, E_3, W_1, B$ the temperature, Reynolds number, non-uniform parameter, Wave number, Hartmann number, Prandtl number, Froude number, Brinkman number, Eckert number, the elasticity parameters and the Powell-Eyring fluid dimensionless parameters respectively.

According to equations (1) and (2) the dimensionless shape of the peristaltic channel walls may be shown in h_1 and h_2

$$h_1(x) = 1 + Mx + a \sin[2\pi(x - t)] \quad (21)$$

$$h_2(x) = -d - Mx - b \sin[2\pi(x - t) + \phi_1] \quad (22)$$

Where (ψ) stream function of velocity components u and v that is dimensionless $u = \frac{\partial \psi}{\partial y}$ and $v = -\frac{\partial \psi}{\partial x}$, respectively and satisfy the continuity equation (10).

In terms of stream function ψ , the dimensionless variables are specified in equations. (11-13) were translated into the following equations.

$$R_e \cdot \delta \left(\frac{\partial \psi}{\partial y \partial t} + \frac{\partial^3 \psi}{\partial x \partial y^2} - \frac{\partial^3 \psi}{\partial x \partial y^2} \right) - \frac{\rho \Omega^2 d_1^2}{\mu} \frac{\partial \psi}{\partial y} + 2\Omega R_e \delta^2 \frac{\partial^2 \psi}{\partial x \partial t} = -\frac{\partial p}{\partial x} + \delta^2 \frac{\partial S_{xx}}{\partial x} + \frac{\partial S_{xy}}{\partial y} - \frac{H^2}{(1+m^2)} \left(\frac{\partial \psi}{\partial y} + \delta m \frac{\partial \psi}{\partial x} \right) + \frac{R_e}{F_r} \sin \alpha \quad (23)$$

$$R_e \cdot \delta^3 \left(-\frac{\partial \psi}{\partial x \partial t} - \frac{\partial^3 \psi}{\partial y \partial x^2} + \frac{\partial^3 \psi}{\partial y \partial x^2} \right) + \frac{\rho \Omega^2 d_1^2}{\mu} \delta^2 \frac{\partial \psi}{\partial x} + 2\Omega R_e \delta^2 \frac{\partial^2 \psi}{\partial y \partial t} = -\frac{\partial p}{\partial y} + \delta^2 \frac{\partial S_{yx}}{\partial x} + \delta \frac{\partial S_{yy}}{\partial y} - \frac{H^2}{(1+m^2)} \delta \left(-\frac{\partial \psi}{\partial x} + m \frac{\partial \psi}{\partial y} \right) - \frac{R_e}{F_r} \delta \cos \alpha \quad (24)$$



$$R_e \cdot \delta \cdot P_r \left(\frac{\partial \theta}{\partial t} + \frac{\partial \theta}{\partial x} \cdot \frac{\partial \psi}{\partial y} - \frac{\partial \theta}{\partial y} \cdot \frac{\partial \psi}{\partial x} \right) = \delta^2 \frac{\partial^2 \theta}{\partial x^2} + \frac{\partial^2 \theta}{\partial y^2} - \delta B_r (S_{xx} - S_{yy}) \frac{\partial^2 \psi}{\partial x \partial y} + B_r S_{xy} \left(\frac{\partial^2 \psi}{\partial y^2} - \delta^2 \frac{\partial^2 \psi}{\partial x^2} \right) + \frac{B_r H^2}{1+m^2} \left(\left(\frac{\partial \psi}{\partial y} \right)^2 + \delta^2 \left(\frac{\partial \psi}{\partial x} \right)^2 \right) \quad (25)$$

Under the assumption of long wavelength approximation ($\delta \ll 1$) and low Reynolds number, eliminate pressure terms using cross differentiation from the dimensionless Equations (23-25) one can write in a single differential equations in terms of stream function ψ as

$$\left(\frac{\rho \Omega^2 d_1^2}{\mu} - \frac{H^2}{(1+m^2)} \right) \frac{\partial^2 \psi}{\partial y^2} + \frac{\partial^2 S_{xy}}{\partial y^2} = 0 \quad (26)$$

$$\frac{\partial^2 \theta}{\partial y^2} + B_r S_{xy} \frac{\partial^2 \psi}{\partial y^2} + \frac{B_r H^2}{(1+m^2)} \left(\frac{\partial \psi}{\partial y} \right)^2 = 0 \quad (27)$$

The axial pressure gradient can be calculated once we've identified the stream function.

$$\frac{\partial p}{\partial x} = \frac{\rho \Omega^2 d_1^2}{\mu} \left(\frac{\partial \psi}{\partial y} \right) + \frac{\partial S_{xy}}{\partial y} - \frac{H^2}{(1+m^2)} \left(\frac{\partial \psi}{\partial y} \right) + \frac{R_e}{F_r} \sin \alpha \quad (28)$$

$$\frac{\partial p}{\partial y} = 0 \quad (29)$$

The dimensionless stress components can be calculated as follows:

$$S_{xx} = 2(1 + W_1) \frac{\partial^2 \psi}{\partial x \partial y} - 2B \left[2\delta^2 \left(\frac{\partial^2 \psi}{\partial y \partial x} \right)^2 + \left(\frac{\partial^2 \psi}{\partial y^2} - \delta^2 \frac{\partial^2 \psi}{\partial x^2} \right)^2 + 2\delta^2 \left(-\frac{\partial^2 \psi}{\partial x \partial y} \right)^2 \right] \frac{\partial^2 \psi}{\partial x \partial y} \quad (30)$$

$$S_{xy} = (1 + W_1) \left(-\delta^2 \frac{\partial^2 \psi}{\partial x^2} + \frac{\partial^2 \psi}{\partial y^2} \right) - B \left[2\delta^2 \left(\frac{\partial \psi}{\partial x \partial y} \right)^2 + \left(-\delta^2 \frac{\partial^2 \psi}{\partial x^2} + \frac{\partial^2 \psi}{\partial y^2} \right)^2 + \delta^2 \left(\frac{\partial^2 \psi}{\partial y \partial x} \right)^2 \right] \left(-\delta^2 \frac{\partial^2 \psi}{\partial x^2} + \frac{\partial^2 \psi}{\partial y^2} \right) \quad (31)$$

$$S_{yy} = -2\delta(1 + W_1) \frac{\partial^2 \psi}{\partial x \partial y} - 2B\delta \left[2\delta^2 \left(\frac{\partial^2 \psi}{\partial x \partial y} \right)^2 + \left(\frac{\partial^2 \psi}{\partial y^2} - \delta^2 \frac{\partial^2 \psi}{\partial x^2} \right)^2 + 2\delta^2 \left(-\frac{\partial^2 \psi}{\partial x \partial y} \right)^2 \right] \frac{\partial^2 \psi}{\partial x \partial y} \quad (32)$$

The corresponding dimensionless boundary conditions are listed below



$$\frac{\partial \psi}{\partial y} \pm \xi \left((1 + W_1) \frac{\partial^2 \psi}{\partial y^2} - B \left(\frac{\partial^2 \psi}{\partial y^2} \right)^3 \right) = 0 \quad \text{at } y = h_1 \text{ and } y = h_2 \quad (33)$$

$$\theta \pm \beta_1 \frac{\partial \theta}{\partial y} = 0 \quad \text{at } y = h_1 \text{ and } y = h_2 \quad (34)$$

$$\left[E_1 \frac{\partial^3}{\partial x^3} + E_2 \frac{\partial^3}{\partial x \partial t^2} + E_3 \frac{\partial^2}{\partial t \partial x} \right] y = \frac{\partial S_{xy}}{\partial y} - \frac{H^2}{(1+m^2)} \left(\frac{\partial \psi}{\partial y} \right) + \frac{R_e}{F_r} \sin \alpha \quad \text{at } y = h_1 \text{ and } y = h_2 \quad (35)$$

$$\text{Heat transfer coefficient at the upper is } Z_1 = \frac{\partial h_1}{\partial x} \cdot \frac{\partial \theta}{\partial y} \quad (36)$$

3. Solution Methodology

The non-linear governing equations are being solved at the present time by means of the perturbation technique for small parameter B . Assume the following flow quantities as

$$\psi = \Psi_0 + B\Psi_1 + \dots \quad (37)$$

$$\theta = \theta_0 + B\theta_1 + \dots \quad (38)$$

3.1 Zero order system and solution

When (26) and (27) are replaced by (37) and (38), which have the same power, the following results are obtained:

$$(1 + W_1) \frac{\partial^4 \Psi_0}{\partial y^4} + \left(\frac{\rho \Omega^2 d_1^2}{\mu} - \frac{H^2}{(1+m^2)} \right) \frac{\partial^2 \Psi_0}{\partial y^2} = 0 \quad (39)$$

$$\frac{\partial^2 \theta_0}{\partial y^2} + B_r (1 + W_1) \left(\frac{\partial^2 \Psi_0}{\partial y^2} \right)^2 + \frac{B_r H^2}{(1+m^2)} \left(\frac{\partial \Psi_0}{\partial y} \right)^2 = 0 \quad (40)$$

where the respective boundary conditions are:

$$\frac{\partial \Psi_0}{\partial y} \pm \xi (1 + W_1) \frac{\partial^2 \Psi_0}{\partial y^2} = 0 \quad \text{at } y = h_1 \text{ and } y = h_2 \quad (41)$$

$$\theta_0 \pm \beta_1 \frac{\partial \theta_0}{\partial y} = 0 \quad \text{at } y = h_1 \text{ and } y = h_2 \quad (42)$$

$$\left[E_1 \frac{\partial^3}{\partial x^3} + E_2 \frac{\partial^3}{\partial x \partial t^2} + E_3 \frac{\partial^2}{\partial t \partial x} \right] y = (1 + W_1) \frac{\partial^3 \Psi_0}{\partial y^3} - \frac{H^2}{(1+m^2)} \left(\frac{\partial \Psi_0}{\partial y} \right) + \frac{R_e}{F_r} \sin \alpha \quad \text{at } y = h_1 \text{ and } y = h_2 \quad (43)$$

The solution the above system for Ψ_0 and θ_0 .



$$\Psi_0 = C_3 + yC_4 + \frac{e^{-\frac{y\sqrt{G^2-R^2}}{\sqrt{1+w_1}}}}{G^2-R^2} \frac{2y\sqrt{G^2-R^2}}{(C_1+e^{-\frac{y\sqrt{G^2-R^2}}{\sqrt{1+w_1}}}} C_2)(1+w_1) \quad (44)$$

$$\theta_0 = r_1 + yr_2 - \frac{B_r L_5}{G^2-R^2} \quad (45)$$

Where $R^2 = \frac{\Omega^2 d_1^2 \rho}{\mu}$, $G^2 = \frac{H^2}{1+m^2}$ and $L_5 = (\frac{1}{2}C_4^2 G^4 y^2 - C_1 C_2 R^2 y^2 -$

$$\begin{aligned} & \frac{1}{2}C_4^2 G^2 R^2 y^2 - C_1 C_2 R^2 y^2 w_1 - \frac{2C_1 C_4 e^{-\frac{\sqrt{G^2-R^2}y}{\sqrt{1+w_1}}}}{\sqrt{G^2-R^2}} \frac{G^2(1+w_1)^{3/2}}{G^2(1+w_1)^{3/2}} + \\ & \frac{2C_2 C_4 e^{-\frac{\sqrt{G^2-R^2}y}{\sqrt{1+w_1}}}}{\sqrt{G^2-R^2}} \frac{G^2(1+w_1)^{3/2}}{G^2(1+w_1)^{3/2}} + \frac{C_1^2 e^{-\frac{2\sqrt{G^2-R^2}y}{\sqrt{1+w_1}}}}{4(G^2-R^2)} \frac{(2G^2-R^2)(1+w_1)^2}{(2G^2-R^2)(1+w_1)^2} + \\ & \frac{C_2^2 e^{-\frac{2\sqrt{G^2-R^2}y}{\sqrt{1+w_1}}}}{4(G^2-R^2)} \frac{(2G^2-R^2)(1+w_1)^2}{(2G^2-R^2)(1+w_1)^2} \end{aligned}$$

3.2. The First Order System and Solution

$$(1 + W_1) \frac{\partial^4 \psi_1}{\partial y^4} + \left(\frac{\rho \Omega^2 d_1^2}{\mu} - \frac{H^2}{(1+m^2)} \right) \frac{\partial^2 \psi_1}{\partial y^2} - \frac{\partial^2}{\partial y^2} \left(\frac{\partial^2 \psi_0}{\partial y^2} \right)^3 = 0 \quad (46)$$

$$\frac{\partial^2 \theta_1}{\partial y^2} + B_r \left(2(1 + W_1) \frac{\partial^2 \psi_0}{\partial y^2} \cdot \frac{\partial^2 \psi_1}{\partial y^2} - \left(\frac{\partial^2 \psi_0}{\partial y^2} \right)^4 \right) + \frac{2 B_r H^2}{1+m^2} \cdot \frac{\partial \psi_0}{\partial y} \cdot \frac{\partial \psi_1}{\partial y} = 0 \quad (47)$$

With the respective boundary conditions are:

$$\frac{\partial \psi_1}{\partial y} \pm \xi \left((1 + W_1) \frac{\partial^2 \psi_1}{\partial y^2} - \left(\frac{\partial^2 \psi_0}{\partial y^2} \right)^3 \right) = 0 \text{ at } y = h_1 \text{ and } y = h_2 \quad (48)$$

$$\theta_1 \pm \beta_1 \frac{\partial \theta_1}{\partial y} = 0 \text{ at } y = h_1 \text{ and } y = h_2 \quad (49)$$

$$(1 + W_1) \frac{\partial^3 \psi_1}{\partial y^3} - \frac{\partial}{\partial y} \left(\frac{\partial^2 \psi_0}{\partial y^2} \right)^3 - \frac{H^2}{1+m^2} \left(\frac{\partial \psi_1}{\partial y} \right) = 0 \text{ at } y = h_1 \text{ and } y = h_2 \quad (50)$$



The solution the above system for Ψ_1 and θ_1

$$\Psi_1 = C7 + yC8 + \frac{L_1+L_2+L_3+L_4}{8\sqrt{G^2-R^2}(1+w_1)}$$

(51)

$$\theta_1 =$$

$$r3 + yr4 +$$

$$\frac{1}{192(G^2-R^2)^2(1+w_1)^{3/2}} e^{-\frac{4\sqrt{G^2-R^2}y}{\sqrt{1+w_1}}} B_r(16C1^3C4e^{\frac{\sqrt{G^2-R^2}y}{\sqrt{1+w_1}}} G^2\sqrt{G^2-R^2}(1+w_1)^2 - 16C2^3C4e^{\frac{7\sqrt{G^2-R^2}y}{\sqrt{1+w_1}}} G^2\sqrt{G^2-R^2}(1+w_1)^2 - 3C1^4(8G^2 - 5R^2)(1+w_1)^{5/2} - 3C2^4e^{\frac{8\sqrt{G^2-R^2}y}{\sqrt{1+w_1}}} (8G^2 - 5R^2)(1+w_1)^{5/2} + 96e^{\frac{4\sqrt{G^2-R^2}y}{\sqrt{1+w_1}}} (G^2 - R^2)y^2(1+w_1)^{3/2}((-9C1^2C2^2 + 2C2C5 + 2C1C6)R^2 + 2C4C8G^2(-G^2 + R^2) + 2(C2C5 + C1C6)R^2w_1) - 96e^{\frac{3\sqrt{G^2-R^2}y}{\sqrt{1+w_1}}} G^2\sqrt{G^2-R^2}(6C1^2C2C4\sqrt{G^2-R^2}y(1+w_1)^{3/2} - (1+w_1)^2(-21C1^2C2C4 + 4C4C5 + 4C1C8 + 4(C4C5 + C1C8)w_1)) - 96e^{\frac{5\sqrt{G^2-R^2}y}{\sqrt{1+w_1}}} G^2\sqrt{G^2-R^2}(6C1C2^2C4\sqrt{G^2-R^2}y(1+w_1)^{3/2} + (1+w_1)^2(-21C1C2^2C4 + 4C4C6 + 4C2C8 + 4(C4C6 + C2C8)w_1)) + 12C1e^{\frac{2\sqrt{G^2-R^2}y}{\sqrt{1+w_1}}} (12C1^2C2\sqrt{G^2-R^2}(2G^2 - R^2)y(1+w_1)^2 + (1+w_1)^{5/2}(C1^2C2(58G^2 - 25R^2) + 8C5(-2G^2 + R^2) + 8C5(-2G^2 + R^2)w_1)) + 12C2e^{\frac{6\sqrt{G^2-R^2}y}{\sqrt{1+w_1}}} (-12C1C2^2\sqrt{G^2-R^2}(2G^2 - R^2)y(1+w_1)^2 + (1+w_1)^{5/2}(C1C2^2(58G^2 - 25R^2) + 8C6(-2G^2 + R^2) + 8C6(-2G^2 + R^2)w_1))))$$

(52)

Where



$$L_1 = \frac{C1^3 e^{-\frac{3y\sqrt{G^2-R^2}}{\sqrt{1+w_1}}}}{\sqrt{G^2-R^2}} (1+w_1), L_2 = \frac{C2^3 e^{-\frac{3y\sqrt{G^2-R^2}}{\sqrt{1+w_1}}}}{\sqrt{G^2-R^2}} (1+w_1),$$

$$L_3 = 2e^{-\frac{y\sqrt{G^2-R^2}}{\sqrt{1+w_1}}} \left(-6C1^2 C2 y \sqrt{1+w_1} + \frac{(1+w_1)(-15C1^2 C2 + 4C5 + 4C5 * w_1)}{\sqrt{G^2-R^2}} \right),$$

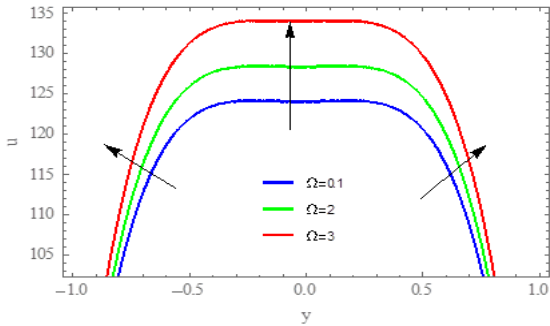
$$L_4 = 2e^{-\frac{y\sqrt{G^2-R^2}}{\sqrt{1+w_1}}} \left(6C1 C2^2 y \sqrt{1+w_1} + \frac{(1+w_1)(-15C1 C2^2 + 4C6 + 4C6 * w_1)}{\sqrt{G^2-R^2}} \right)$$

4. Results and Discussions

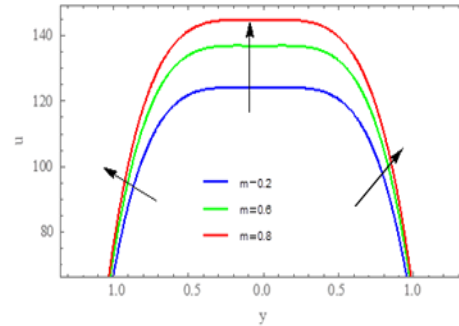
The analysis of (the axial velocity) u , (temperature) θ , Heat transfer coefficient Z_1 and (stream function) ψ are determined in this section.

4.1 Velocity behavior "u"

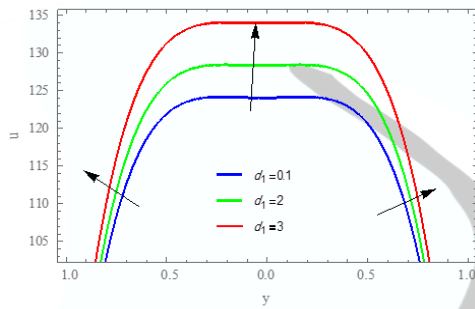
We will now examine the impact of the axial velocity (u) variation across the channel on a number of different factors. According to Figures 2 (a-i) as the rotation parameter Ω , Hall parameter m , the width of the channel d_1 , wall properties parameter $E1, E2, E3$, the non-uniform parameter M , the channel inclination angle α and the phase difference ϕ_1 are varied, the axial velocity rises in the center and towards the channel wall. Figures 2 (j and k) show how the axial velocity increases in the middle of the channel and decreases towards the channel wall as Reynolds number Re and material parameters of Powell-Erying fluid B , while Figures 2(l - n) show how the axial velocity decreases in the center of the channel and increases at the wall border when the Hartmann number H , material parameters of Powell-Erying fluid W_1 and Froude number Fr are changed. Figures 2 (o) the axial velocity decreases in the center and toward the channel wall where the velocity slip parameter ξ increases. Because the fluid is incompressible, the axial velocity in Figure 2(p and q) is unaffected by the viscosity μ and density ρ .



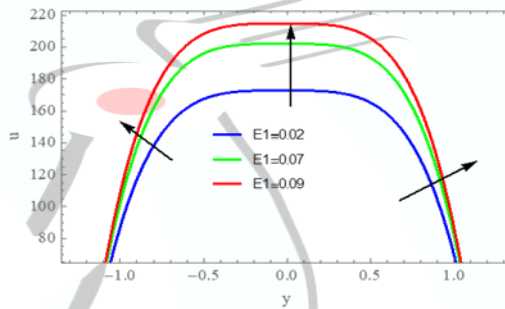
(a)



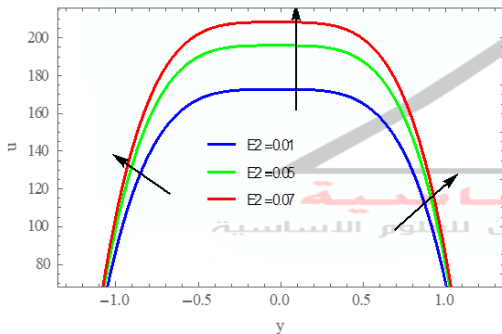
(b)



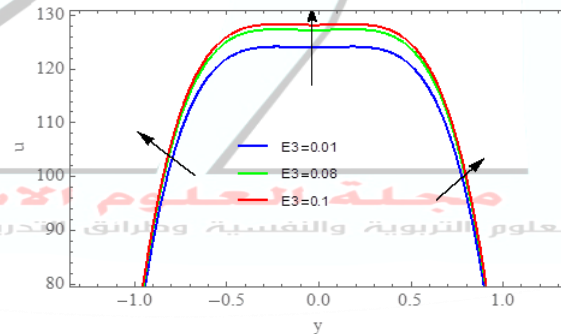
(c)



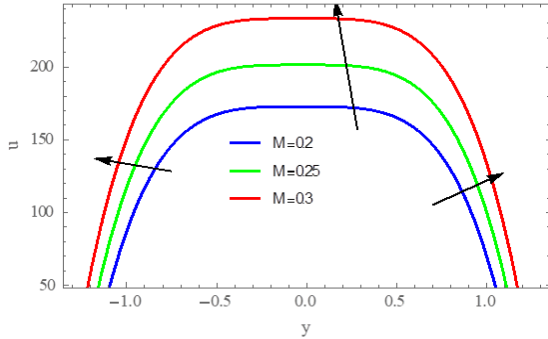
(d)



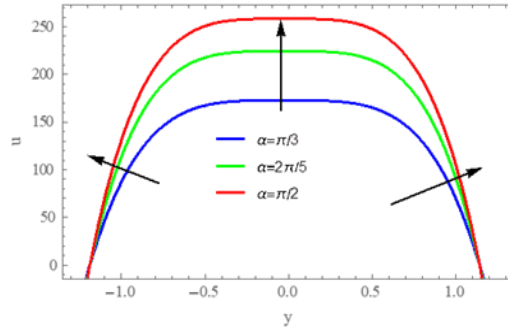
(e)



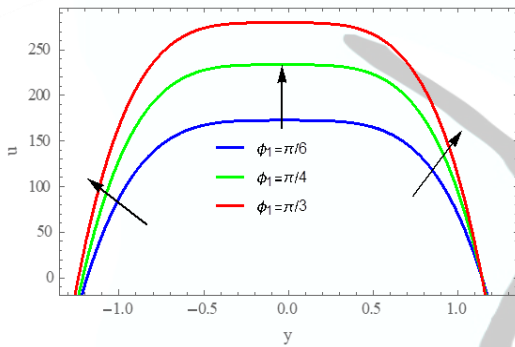
(f)



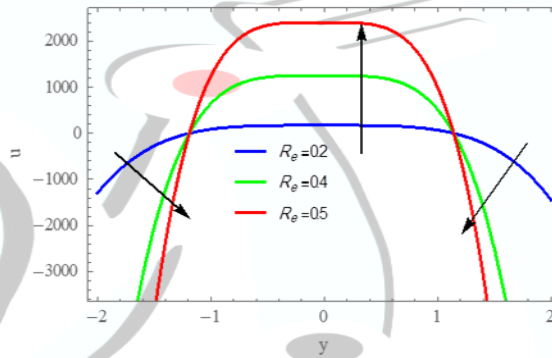
(g)



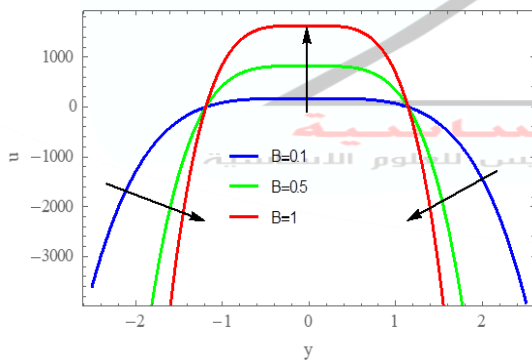
(h)



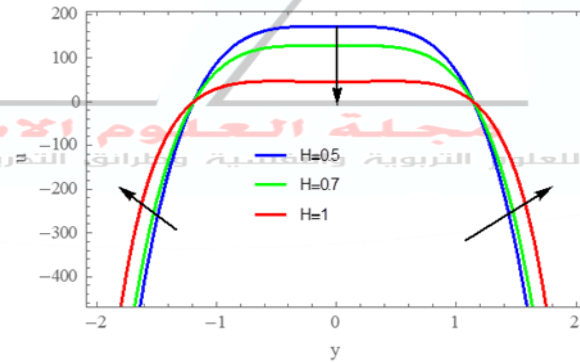
(i)



(j)



(k)



(l)

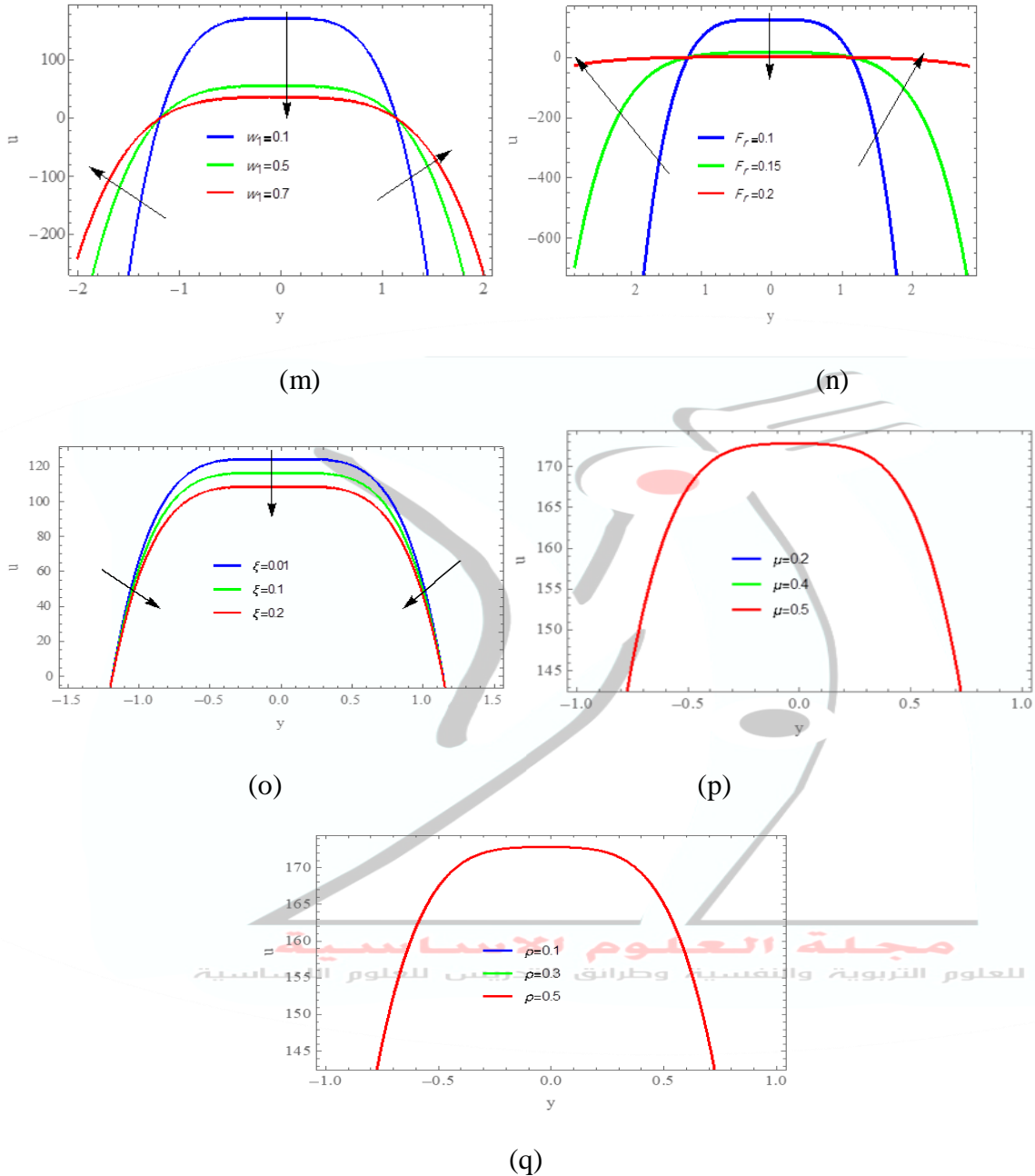
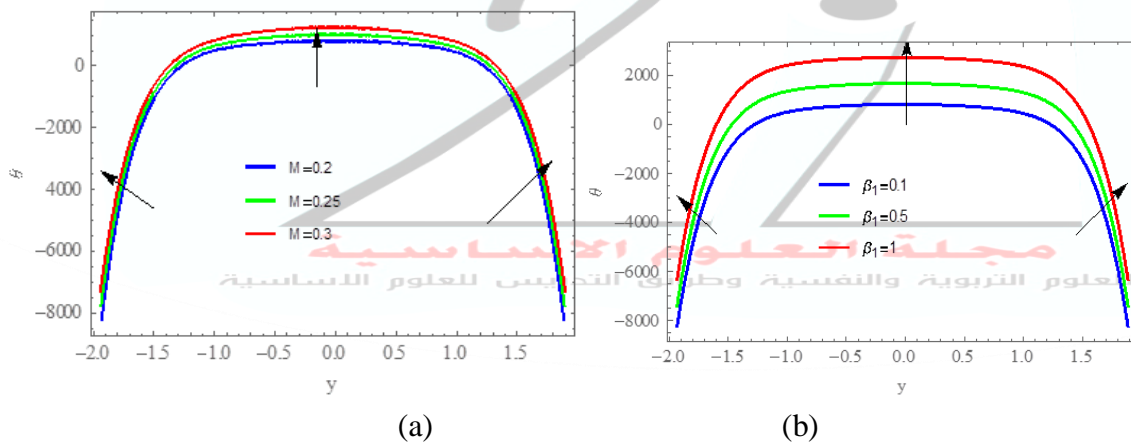


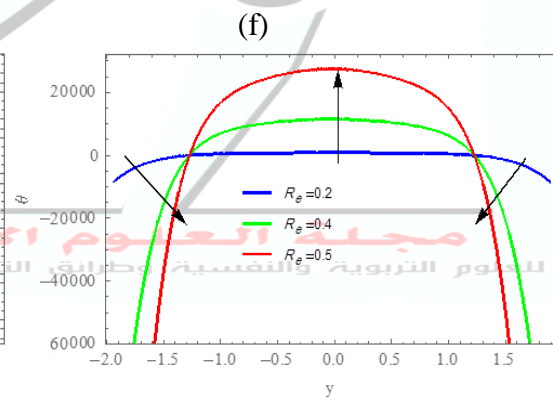
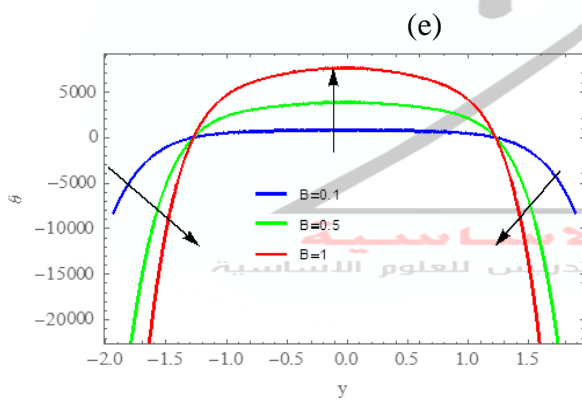
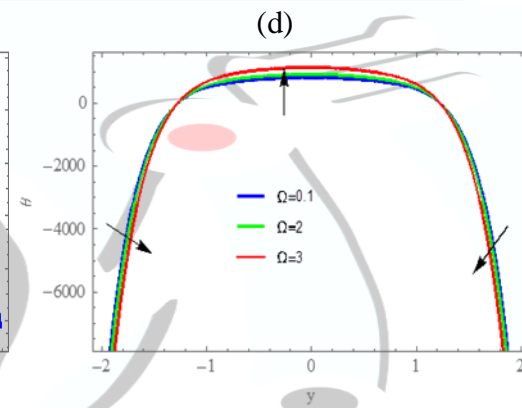
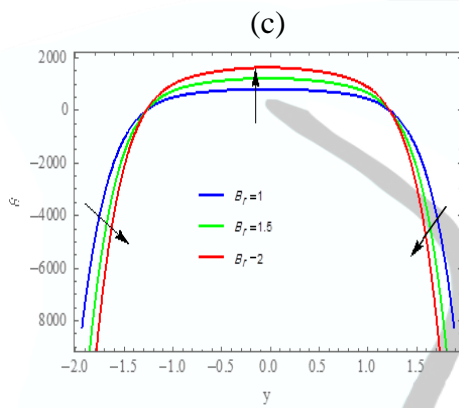
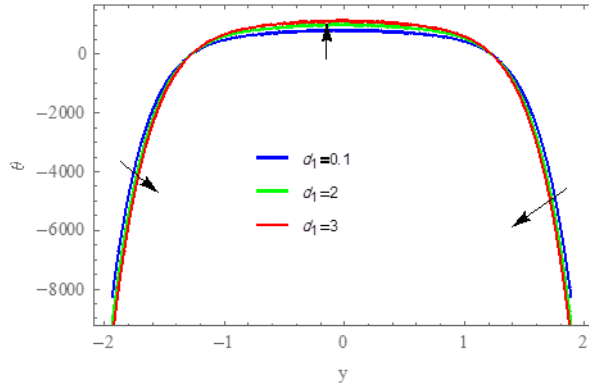
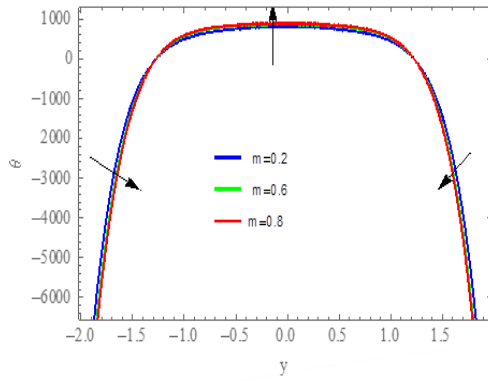
Figure 2- Variation the axial velocity u with different perimeters $a = 0.1, b = 0.1, M = 0.2, \Omega = 0.1, d_1 = 0.1, \rho = 0.1, d = 0.01, \mu = 0.2, H = 0.5, m = 0.2, E1 = 0.02, E2 = 0.01, W_1 = 0.1, B = 0.1, E3 = 0.01, t = 0.1, R_e = 0.2, \xi = 0.01, \phi_1 = \pi/6, \alpha = \pi/3, F_r = 0.1, x = 1$



4.2 Temperature Behavior " θ "

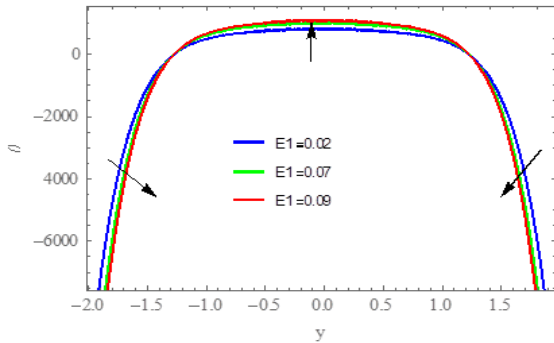
An analysis of the temperature distribution of a fluid with a constant value of $x = 1$ and $t = 0.1$. The effect of different parameters on temperature distribution is shown in Figures 3 (a and b) as the non-uniform parameter M and thermal slip parameter β_1 are varied, the temperature rises in the center. Figures 3 (c and l) show how the temperature increases in the center of the channel and decreases towards the channel wall as Hall parameter m , the width of the channel d_1 , B_r , the rotation parameter Ω , material parameters of fluid B , R_e , wall properties parameter E_1, E_2, E_3 and the channel inclination angle α . According to Figure 3(m) the phase difference ϕ_1 , is shown to increase the temperature in the middle of the channel while the temperature lowers at one wall boundary and rises at the other. The temperature in Figure 3(n and o) is unaffected by the viscosity μ and density ρ . When the velocity slip parameter ξ , fluid material parameters W_1, F_r and the Hartmann number H are changed, the temperature decreases in the center of the channel and increases at the wall border, as shown in Figures 3(p-s).



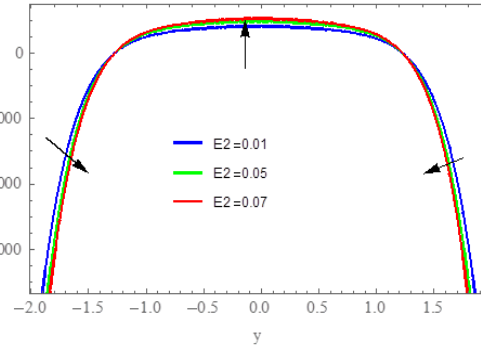


(g)

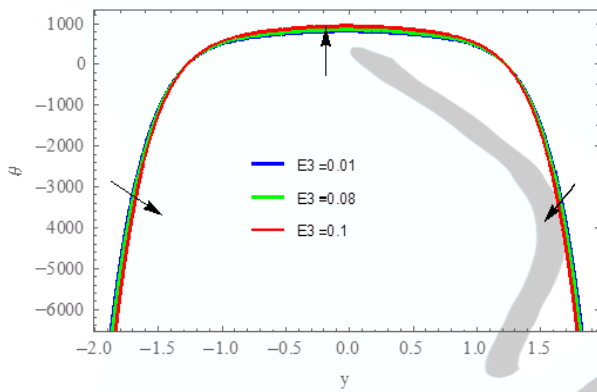
(h)



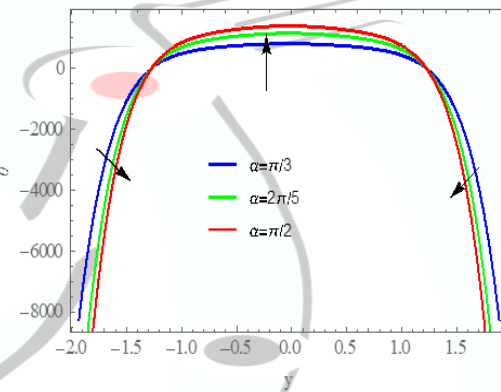
(i)



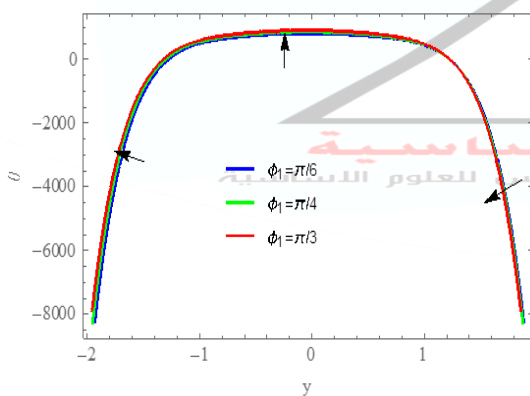
(j)



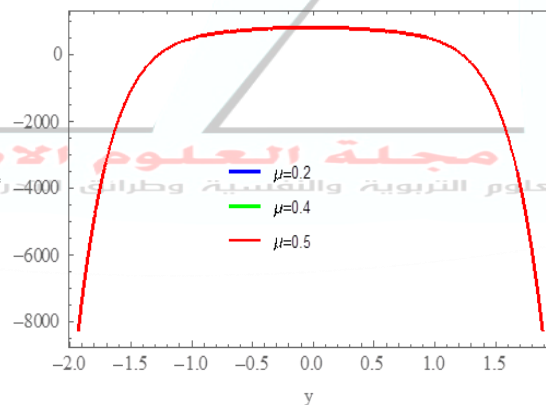
(k)



(l)



(m)



(n)

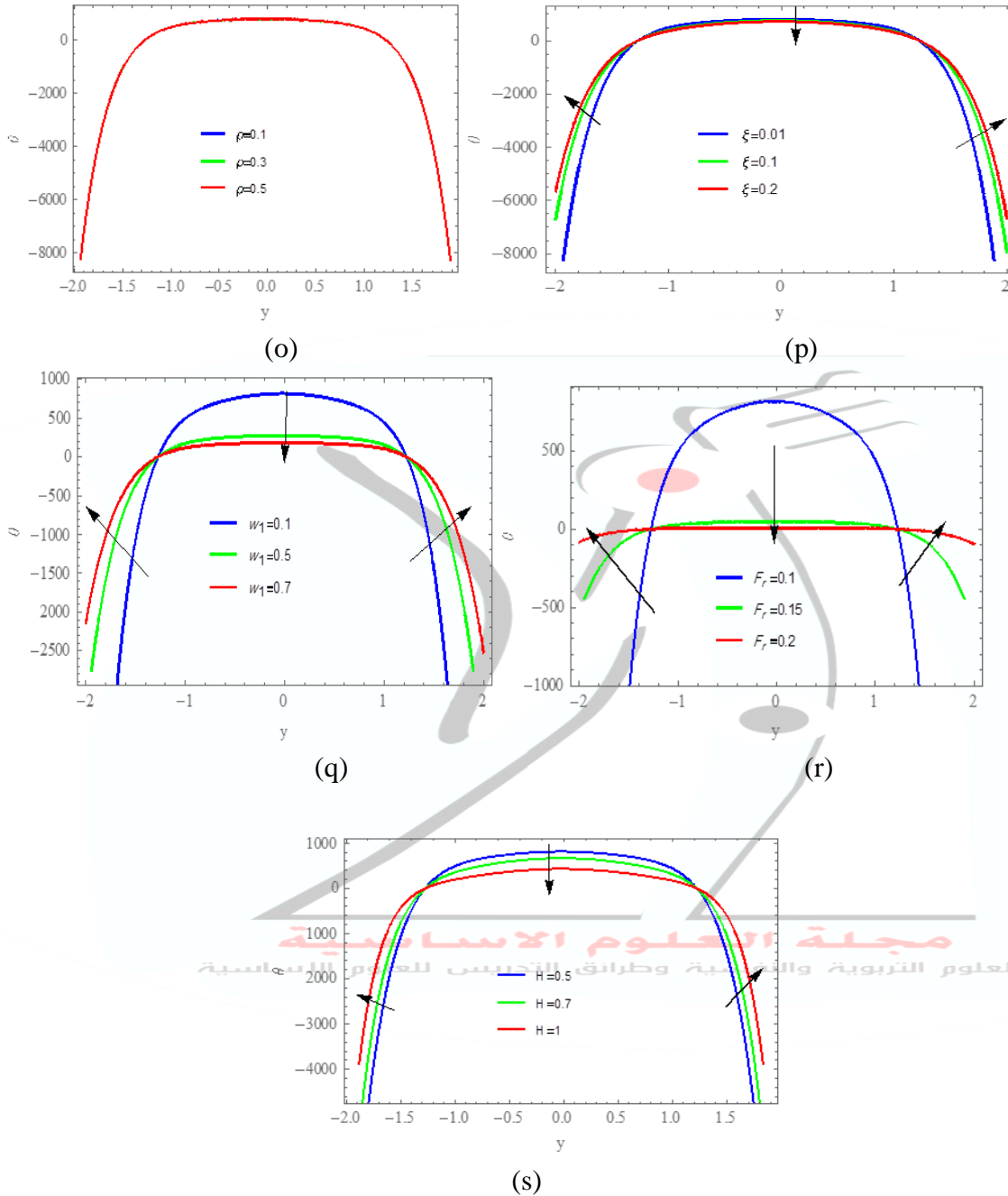
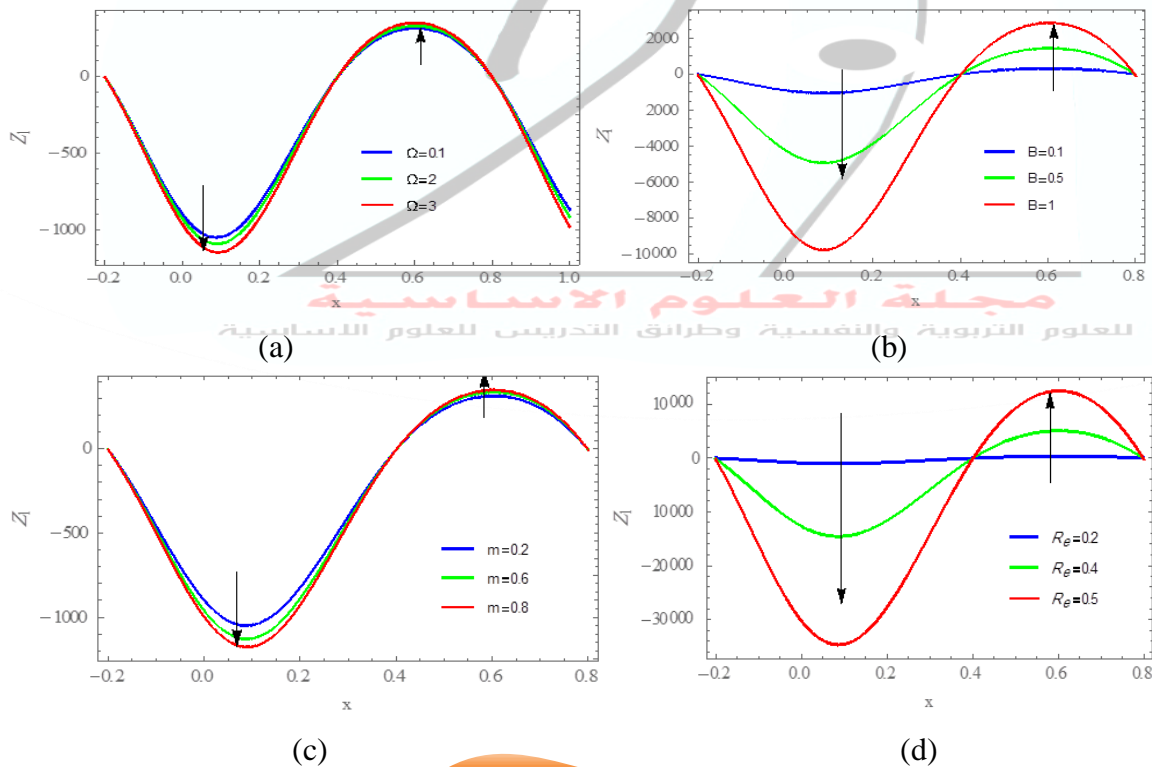


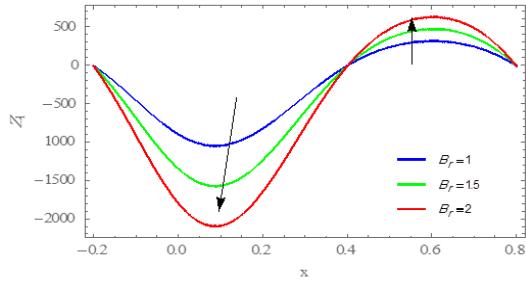
Figure 3- Variation the temperature θ with different perimeters $\{a = 0.1, b = 0.1, M = 0.2, \Omega = 0.1, d_1 = 0.1, \rho = 0.1, d = 0.01, \mu = 0.2, H = 0.5, m = 0.2, E1 = 0.02, E2 = 0.01, W_1 = 0.1, B = 0.1, E3 = 0.01, t = 0.1, R_e = 0.2, \xi = 0.01, \phi_1 = \pi/6, \alpha = \pi/3, F_r = 0.1, \beta_1 = 0.1, B_r = 1, x = 1\}$



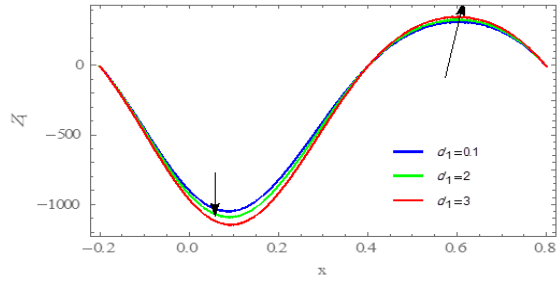
4.3 Heat Transfer Coefficient

In this section, we looked at a number of parameters to see how they affect the heat transfer coefficient (Z_1). In the right conditions, the heat transfer coefficient (Z_1) on the upper wall will move back and forth in an oscillating pattern. due to peristaltic waves getting smaller and bigger along the walls of the channel. As seen in Figures 4 (a–g), the heat transfer coefficient (Z_1) goes up as Ω , B , m , R_e , B_r , d_1 and α go up. Figures 4 (h–k) show that the heat transfer coefficient Z_1 decreases as H increases due to the existence of a magnetic field, W_1 , F_r and ξ increase. According to Figures 4 (l–n) M , $E1$ and $E2$ are shown mixed behavior. According to Figure 4(o) $E3$ is shown to increase the heat transfer coefficient in the middle of the channel while the heat transfer coefficient is upper at one wall boundary and rises at the other. The heat transfer coefficient in Figure 4(p– r) is unaffected by μ , β_1 and ρ .

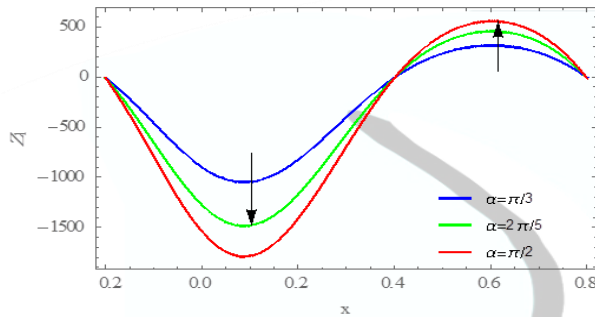




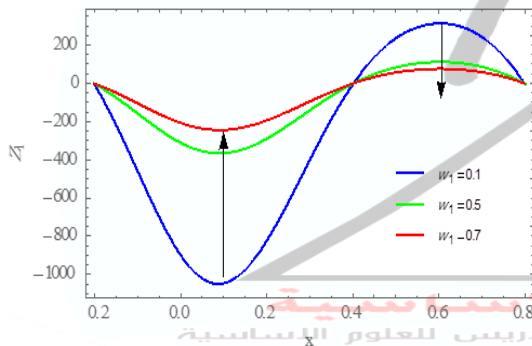
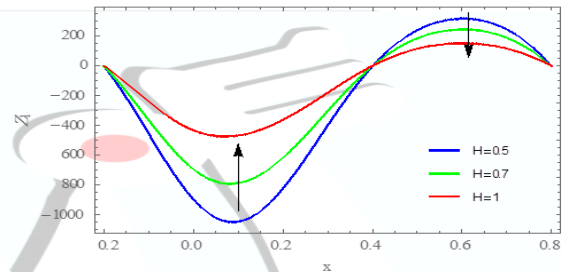
(e)



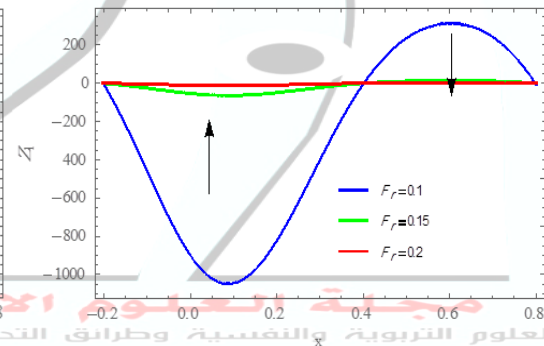
(f)



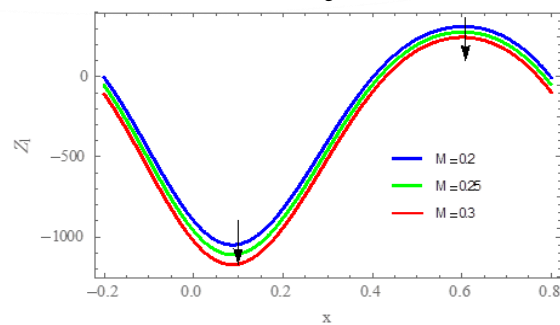
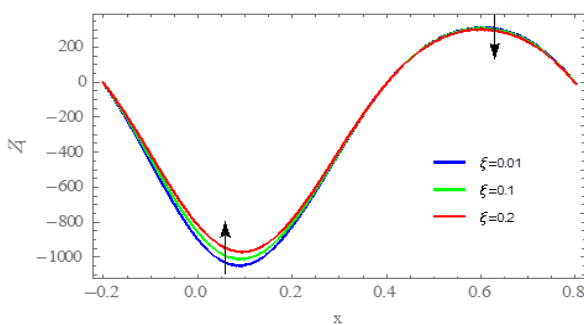
(g)



(i)



(j)



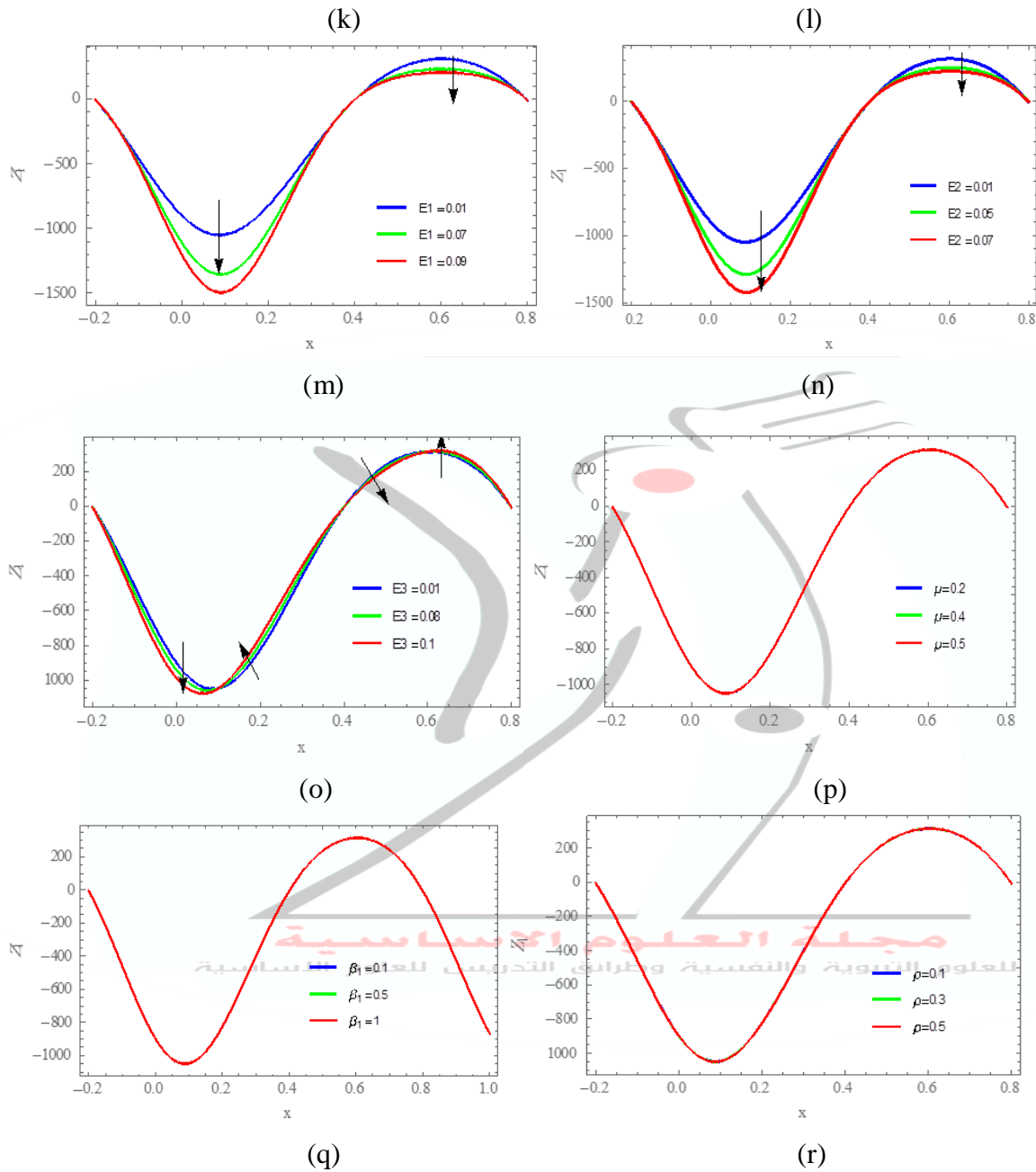


Figure 4- Variation heat transfer coefficient(Z_1) different perimeters{ $a = 0.1, b = 0.1, M = 0.2, \Omega = 0.1, d_1 = 0.1, \rho = 0.1, d = 0.01, \mu = 0.2, H = 0.5, m = 0.2, E_1 =$



$0.02, E2 = 0.01, W_1 = 0.1, B = 0.1, E3 = 0.01, t = 0.1, R_e = 0.2, \xi = 0.01, \phi_1 = \pi/6, \alpha = \pi/3, F_r = 0.1, \beta_1 = 0.1, B_r = 1, y = 1\}$

4.4. The trapping phenomena

Various effective parameters' effects on streamlines for a fixed time $t=0.1$ are provided in this section's Figs (5- 17). Trapping, which is the term for the emergence of a remarkable occurrence in peristaltic motion, is an internal-circulating bolus of fluid that travels in time with the peristaltic waves with waves. The drawings indicate that the bolus looks close to all of the upper and lower walls. Figure (5) illustrates how the size of the trapped bolus decreases as the Hartman number H rises, and this happens because the Lorentz force opposes the fluid flow. Figures (6-8) show the size and number of the trapped bolus decreases as the fluid parameter B , the velocity slip parameter ξ and Reynolds number R_e rises, while the figures(9-14) show that the size and number of the trapped bolus increases with the increase of each the Hall parameter m , the rotation parameter Ω , Froude number F_r , material parameters of Powell-Erying fluid W_1 , the non-uniform parameter M and the width of the channel d_1 . According to Figure (15) is shown that the size of the trapped bolus increases with the increase wall properties parameter $E1$, $E2$ and $E3$ by increasing it, the size of the entrapped bolus decreases. Figures (16 and 17) illustrates how the size of the trapped bolus is not effect when change values of ρ and μ .

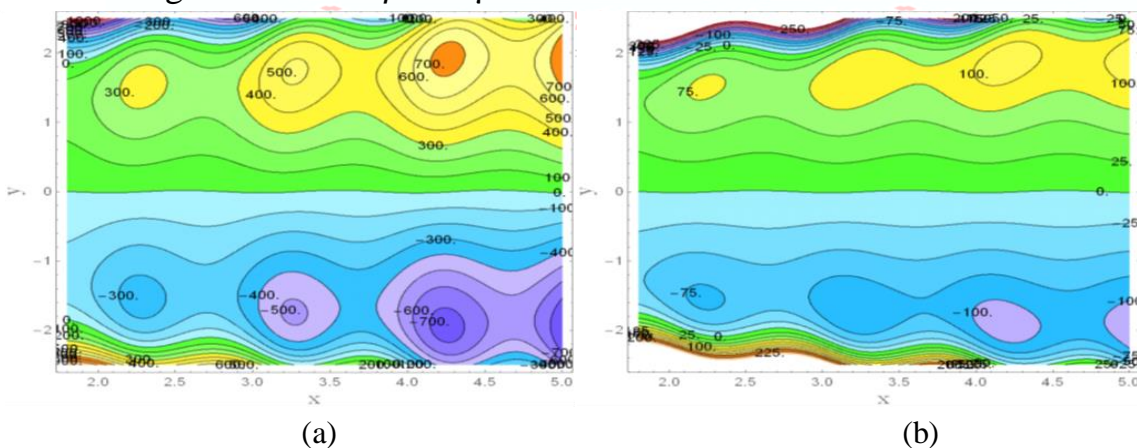


Figure 5- Effect via H on ψ for $a = 0.1, b = 0.1, M = 0.2, \Omega = 0.1, d_1 = 0.1, \rho = 0.1, d = 0.01, \mu = 0.2, m = 0.2, E1 = 0.02, E2 = 0.01, E3 = 0.01, W_1 = 0.1, B = 0.1, t = 0.1, R_e = 0.2, \xi = 0.01, \phi_1 = \pi/6, \alpha = \pi/3, F_r = 0.1$ when (a) $H = 0.5$ (b) $H = 1$

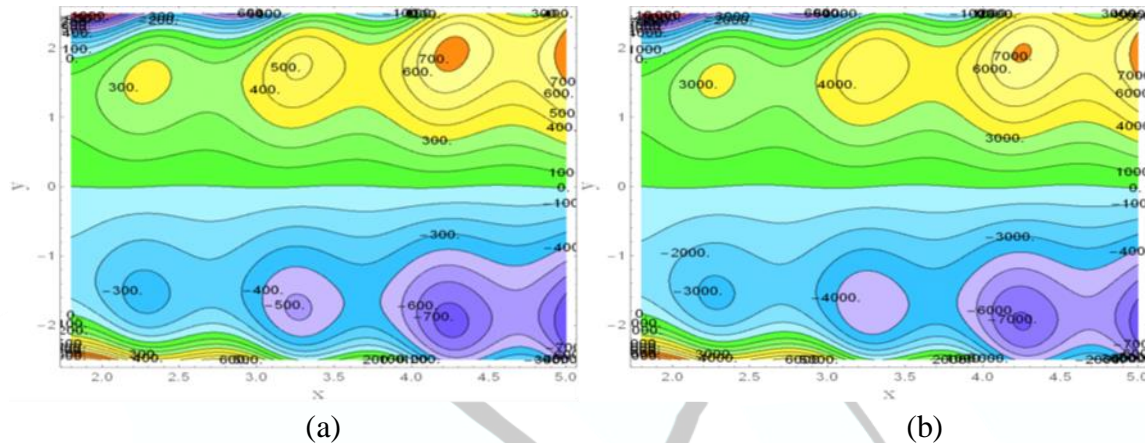


Figure 6- Effect via B on ψ for $a = 0.1, b = 0.1, H = 0.5, \Omega = 0.1, d_1 = 0.1, \rho = 0.1, \mu = 0.2, d = 0.01, m = 0.2, E1 = 0.02, E2 = 0.01, E3 = 0.01, W_1 = 0.1, M = 0.2, t = 0.1, R_e = 0.2, \xi = 0.01, \phi_1 = \pi/6, \alpha = \pi/3, F_r = 0.1$ when (a) $B = 0.1$ (b) $B = 1$

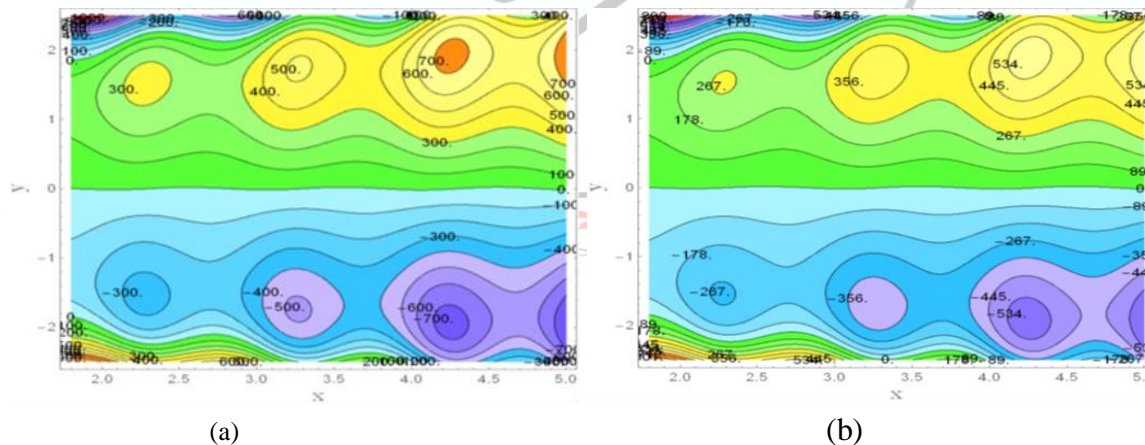


Figure 7- Effect via ξ on ψ for $\{ a = 0.1, b = 0.1, M = 0.2, \Omega = 0.1, d_1 = 0.1, \rho = 0.1, d = 0.01, \mu = 0.2, H = 0.5, E1 = 0.02, E2 = 0.01, E3 = 0.01, W_1 = 0.1, B = 0.1, t = 0.1, R_e = 0.2, m = 0.2, \phi_1 = \pi/6, \alpha = \pi/3, F_r = 0.1 \}$ when (a) $\xi = 0.01$ (b) $\xi = 0.2$

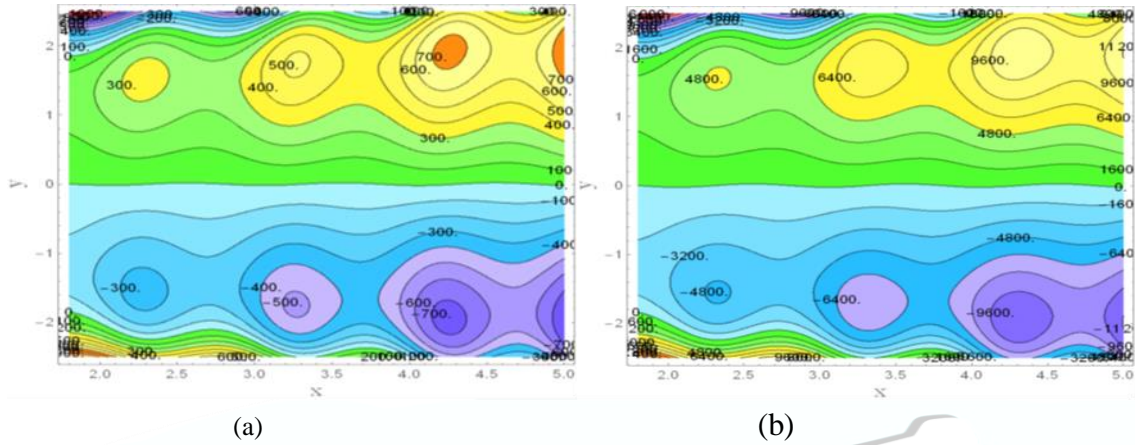


Figure 8- Effect via R_e on ψ for $a = 0.1, b = 0.1, M = 0.2, \Omega = 0.1, d_1 = 0.1, \rho = 0.1, d = 0.01, \mu = 0.2, H = 0.5, m = 0.2, E1 = 0.02, E2 = 0.01, E3 = 0.01, B = 0.1, t = 0.1, W_1 = 0.1, \xi = 0.01, \phi = \pi/6, \alpha = \pi/3, Fr = 0.1$ when (a) $R_e = 0.2$ (b) $R_e = 0.5$

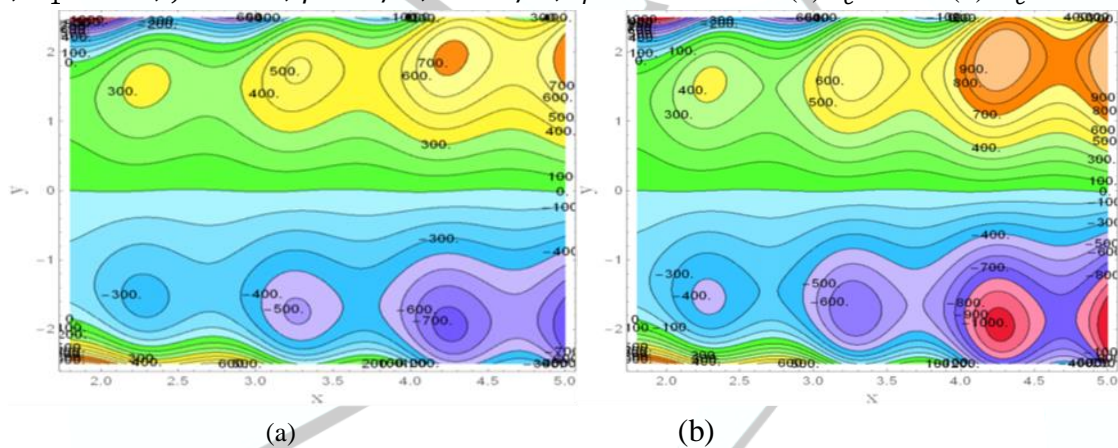
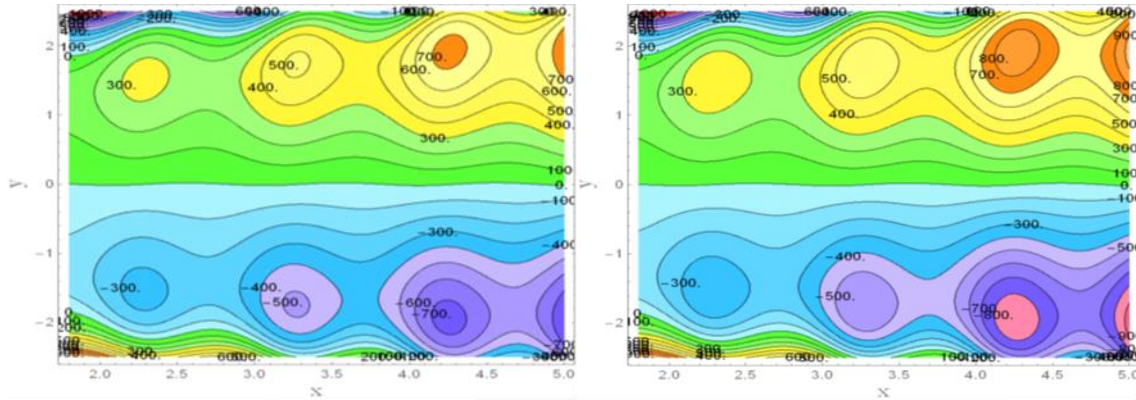


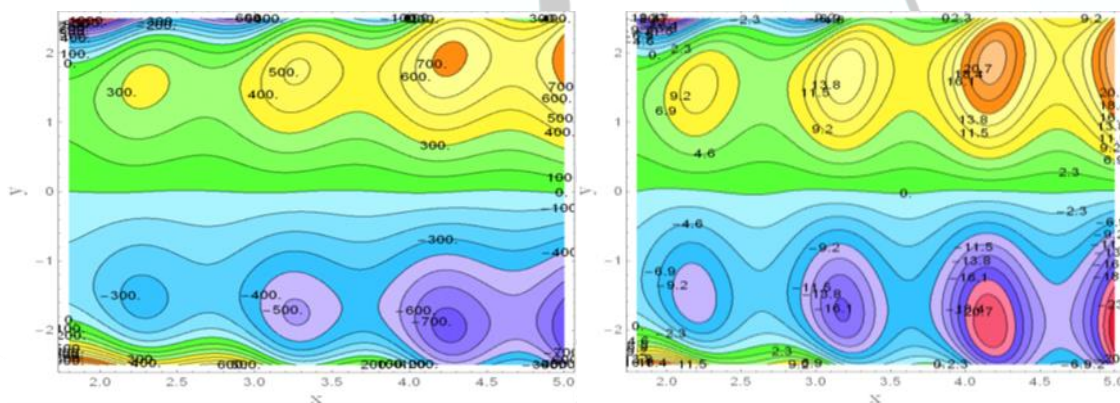
Figure 9- Effect via m on ψ for $a = 0.1, b = 0.1, M = 0.2, W_1 = 0.1, d_1 = 0.1, \rho = 0.1, d = 0.01, \mu = 0.2, H = 0.5, B = 0.1, E1 = 0.02, E2 = 0.01, E3 = 0.01, \Omega = 0.1, t = 0.1, R_e = 0.2, \xi = 0.01, \phi = \pi/6, \alpha = \pi/3, Fr = 0.1$ when (a) $m = 0.2$ (b) $m = 0.8$



(a)

(b)

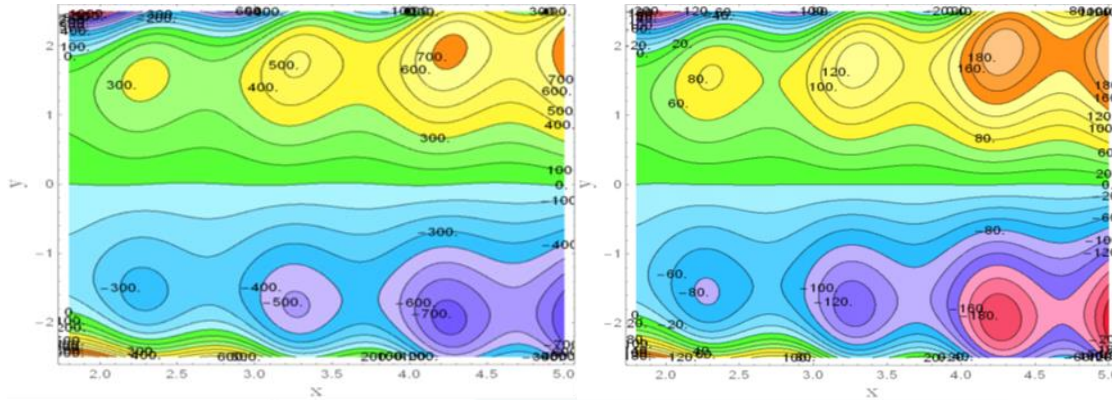
Figure 10-Effect via Ω on ψ for $a = 0.1, b = 0.1, M = 0.2, W_1 = 0.1, d_1 = 0.1, \rho = 0.1, d = 0.01, \mu = 0.2, H = 0.5, m = 0.2, E1 = 0.02, E2 = 0.01, E3 = 0.01, B = 0.1, t = 0.1, R_e = 0.2, \xi = 0.01, \phi = \pi/6, \alpha = \pi/3, F_r = 0.1$ when (a) $\Omega = 0.1$ (b) $\Omega = 3$



(a)

(b)

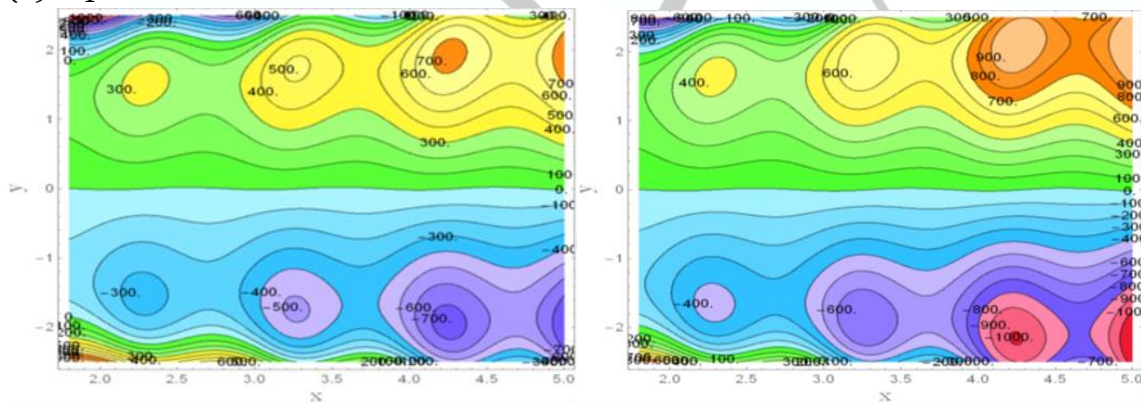
Figure 11-Effect via F_r on ψ for $a = 0.1, b = 0.1, M = 0.2, W_1 = 0.1, d_1 = 0.1, \rho = 0.1, d = 0.01, \mu = 0.2, H = 0.5, m = 0.2, E1 = 0.02, E2 = 0.01, E3 = 0.01, \Omega = 0.1, t = 0.1, R_e = 0.2, \xi = 0.01, \phi = \pi/6, \alpha = \pi/3, B = 0.1$ when (a) $F_r = 0.1$ (b) $F_r = 0.2$



(a)

(b)

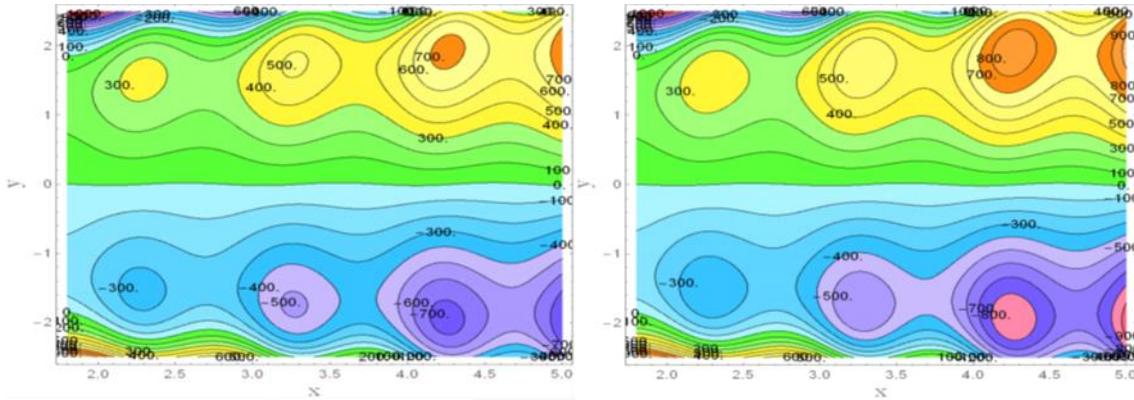
Figure 12-Effect via W_1 on ψ for $a = 0.1, b = 0.1, M = 0.2, \xi = 0.01, d_1 = 0.1, \rho = 0.1, d = 0.01, \mu = 0.2, H = 0.5, m = 0.2, E1 = 0.02, E2 = 0.01, E3 = 0.01, \Omega = 0.1, t = 0.1, Re = 0.2, Fr = 0.1, \phi = \pi/6, \alpha = \pi/3, B = 0.1$ when (a) $W_1 = 0.1$ (b) $W_1 = 0.7$



(a)

(b)

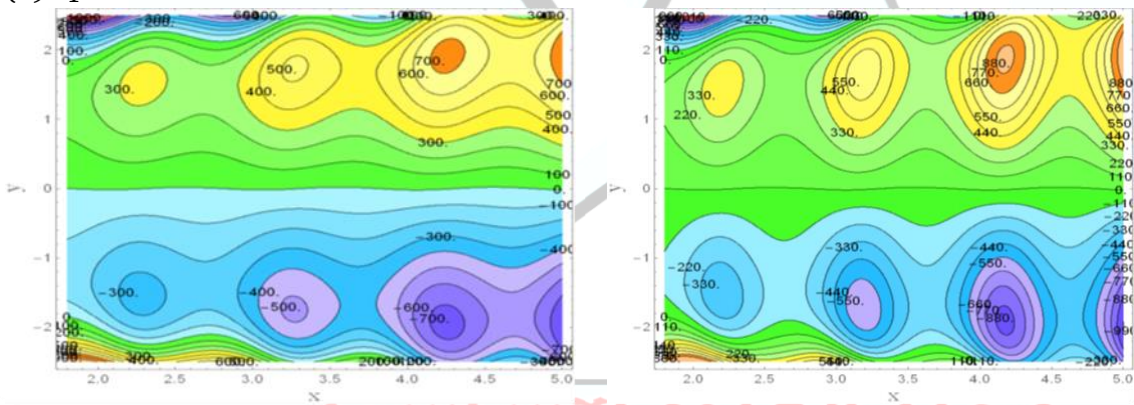
Figure 13-Effect via M on ψ for $a = 0.1, b = 0.1, Re = 0.2, W_1 = 0.1, d_1 = 0.1, \rho = 0.1, d = 0.01, \mu = 0.2, H = 0.5, m = 0.2, E1 = 0.02, E2 = 0.01, E3 = 0.01, \Omega = 0.1, t = 0.1, \xi = 0.01, Fr = 0.1, \phi = \pi/6, \alpha = \pi/3, B = 0.1$ when (a) $M = 0.2$ (b) $M = 0.3$



(a)

(b)

Figure 14-Effect via d_1 on ψ for $a = 0.1, b = 0.1, R_e = 0.2, W_1 = 0.1, M = 0.1, \rho = 0.1, d = 0.01, \mu = 0.2, H = 0.5, m = 0.2, E_1 = 0.02, E_2 = 0.01, E_3 = 0.01, \Omega = 0.1, t = 0.1, \xi = 0.01, F_r = 0.1, \phi = \pi/6, \alpha = \pi/3, B = 0.1$ when (a) $d_1 = 0.1$ (b) $d_1 = 3$



(a)

(b)

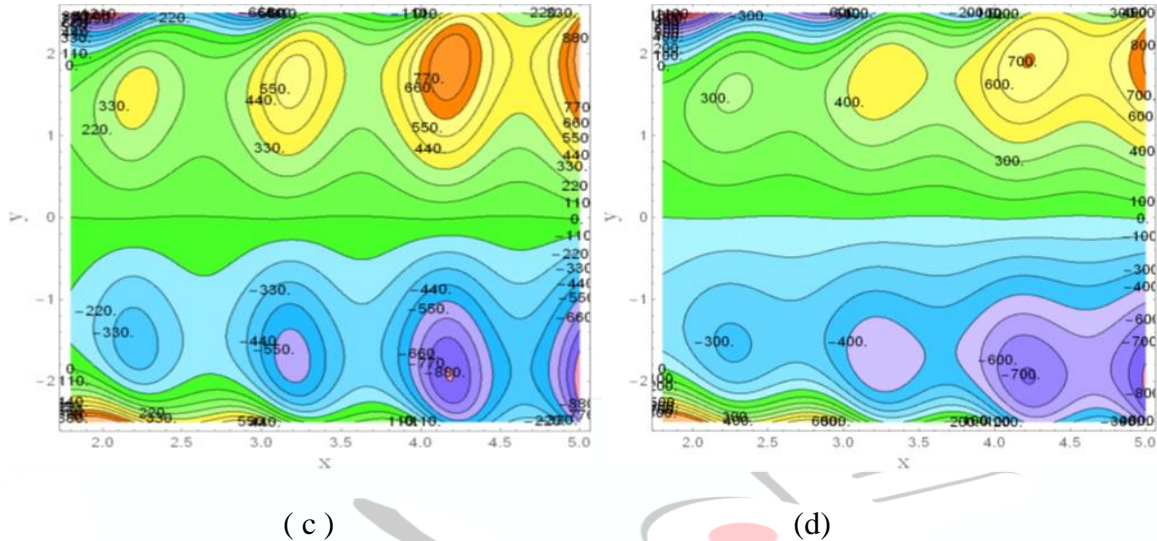


Figure 15-Effect via wall properties on ψ for $a = 0.1, b = 0.1, M = 0.2, W_1 = 0.1, d_1 = 0.1, \rho = 0.1, d = 0.01, \mu = 0.2, H = 0.5, m = 0.2, R_e = 0.2, \Omega = 0.1, t = 0.1, \xi = 0.01, F_r = 0.1, \phi_1 = \pi/6, \alpha = \pi/3, B = 0.1$ when (a) $E1 = 0.02, E2 = 0.01, E3 = 0.01$ (b) $E1 = 0.09, E2 = 0.01, E3 = 0.01$ (c) $E1 = 0.02, E2 = 0.07, E3 = 0.01$ (d) $E1 = 0.02, E2 = 0.01, E3 = 0.1$

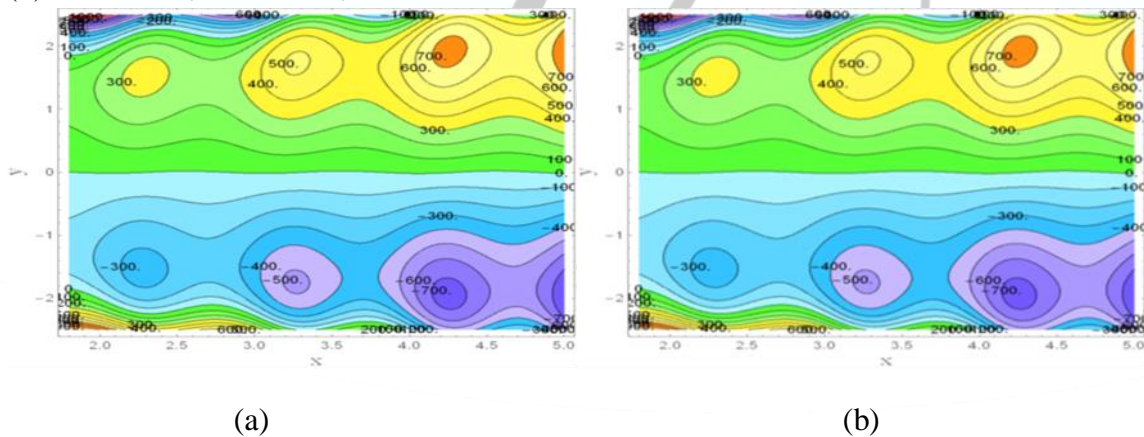


Figure 16 -Effect via ρ on ψ for $a = 0.1, b = 0.1, M = 0.2, W_1 = 0.1, d_1 = 0.1, \mu = 0.2, R_e = 0.2, d = 0.01, H = 0.5, m = 0.2, E1 = 0.02, E2 = 0.01, E3 = 0.01, \Omega = 0.1, t = 0.1, \xi = 0.01, F_r = 0.1, \phi = \pi/6, \alpha = \pi/3, B = 0.1$ when (a) $\rho = 0.1$ (b) $\rho = 0.5$

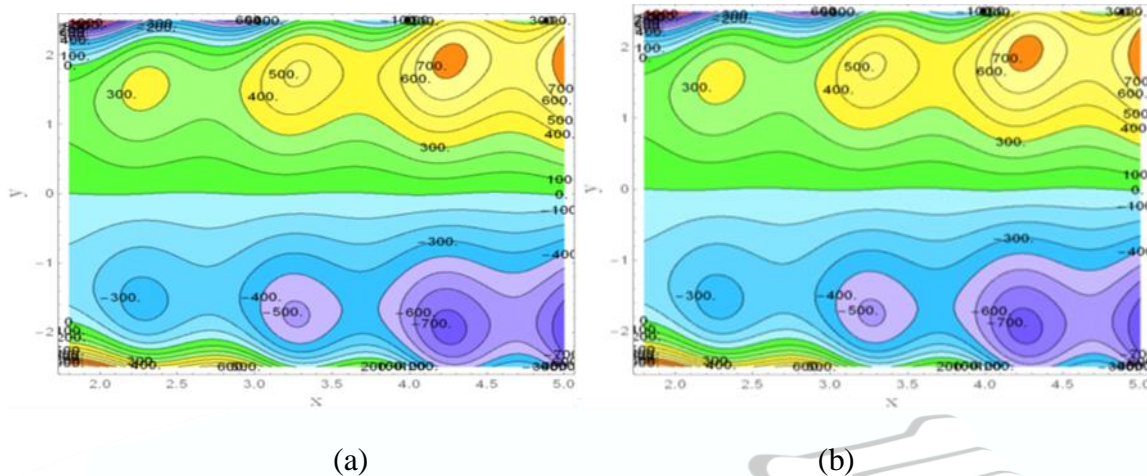


Figure 17-Effect via μ on ψ for $a = 0.1, b = 0.1, M = 0.2, W_1 = 0.1, d_1 = 0.1, \rho = 0.1, R_e = 0.2, d = 0.01, H = 0.5, m = 0.2, E1 = 0.02, E2 = 0.01, E3 = 0.01, \Omega = 0.1, t = 0.1, \xi = 0.01, F_r = 0.1, \phi = \pi/6, \alpha = \pi/3, B = 0.1$ when (a) $\mu = 0.2$ (b) $\mu = 0.5$

6. Conclusions

In this study, we investigated the effects of rotation with Hall and Joule heating on a Powell-Eyring fluid's ability to transmit heat via an inclined, tapered, asymmetrical channel while operating under low Reynolds approximations and long-wavelength assumptions. The traditional perturbation method has been used to find analytical solutions. The following are the key considerations of the analysis:

1. The qualitatively contrasting effects of Powell-Eyring fluid parameters W_1 and B in trapped streamlines, the axial velocity, temperature and heat transfer coefficient are considered.
2. The viscosity μ and density ρ have no impact on the axial velocity, temperature, heat transfer coefficient and trapped streamlines. because the fluid is incompressible.
3. Hall parameter m and Hartmann number H have an opposing influence in trapped streamlines, the axial velocity, temperature and heat transfer coefficient.



4. There is an increase in axial velocity " u " in the central region when increasing the rotation parameter Ω , $m, d_1, E1, E2, E3, M, \alpha, \phi_1$, While it increases in the central region and decreases at the canal border when increasing the fluid parameters B and R_e
5. The axial velocity " u " rises in the central region when increasing ξ , While it increases in the central region and decreases at the canal border when increasing H, W_1 and F_r .
6. The temperature " θ " rises in the central region when increasing M, β_1 , While it increases in the central region and decreases at the canal border when increasing the fluid parameters $B, R_e, B_r, \Omega, m, d_1, E1, E2, E3$, and α .
7. There is a decrease in temperature " θ " in the central region when increasing H, W_1, F_r, ξ , but there is a rise in temperature at the boundary of the channel wall.
8. All embedded parameters exhibit oscillating behavior depending on the heat transfer coefficient Z_1 magnitude.
9. The size of the trapped bolus in the tapered asymmetric channel grows as the Hall parameter $m, \Omega, E1, E2, W_1, F_r, M, d_1$ goes up, while its size go down as the Hartman number $H, E3, \xi, B, R_e$ goes up.

References

1. Ali, H.A. & Abdulhadi, A.M. (2018). Analysis of heat transfer on peristaltic transport of Powell-Eyring fluid in an inclined tapered symmetric channel with Hall and Ohm's heating influences. *Journal of Al-Qadisiyah for computer science & mathematics*, 10(2), 26-41.
2. Alshareef, T. Sh. (2020). Impress of rotation and an inclined MHD on waveform motion of the nonNewtonian fluid through porous canal. *Journal of Physics: Conference Series*, 1591, IOP Publishing.
3. Asfour, H.A. –H. (2020). The effects of Joule heating and variable thermal conductivity on peristaltic pumping of Jeffrey nanofluid in the presence of heat transfer. *Heat Transfer*, 49 (3), 1237-1255.



4. Abdulhussein, H. & Abdalhadi, A.M. (2022). Impact of couple stress and rotation on peristaltic transport of a Powell-Eyring fluid in an inclined asymmetric channel with Hall and joule heating. *Journal of Basic Sciences*, 8(13), 483-509: <http://bsj.uowasit.edu.iq>
5. Hasen, S.S., Kareem, R.S. & Ali, H.A. (2022). Mathematical analysis of peristaltic pumps for Fene-P model subject to Hall and Joule impact. *Iraqi Journal of Science*, 63(7), 3141-3152.
6. Hassen, R.Y. & Ali, H.A. (2021). Hall and Joule's heating influences on peristaltic transport of Bingham plastic fluid with variable viscosity in an inclined tapered asymmetric channel. *Ibn AL-Haitham Journal for Pure and Applied Sciences*, 34(1), 68-84.
7. Hayat, T., Naseema, A., Rafiq M. & Fuad, E.A. (2017). Hall and Joule heating effects on peristaltic flow of Powell–Eyring liquid in an inclined symmetric channel. *Results in Physics*, 7, 518–528.
8. Hina, S. (2016). MHD peristaltic transport of Eyring- Powell fluid with heat/mass transfer, wall properties and slip conditions. *Journal of Magnetism and Magnetic Materials*, 404, 148-158.
9. Mohaisen, H.N. & Abdalhadi, A.M. (2021). Effects of The Rotation and A Magnetic Field on The Mixed Convection Heat Transfer Analysis for The Peristaltic Transport of Viscoplastic Fluid Through a Porous Medium in Asymmetric Channel. *Journal of Physics: Conference Series*, 1963(1), 012165, IOP Publishing.
10. Murad, M.A. & Abdalhadi, A.M. (2020). Influence of MHD on mixed convective heat and mass transfer analysis for the peristaltic transport of viscoplastic fluid with porous medium in tapered channel. *Journal of Al-Qadisiyah for computer Science & Mathematics*, 12 (4), 79-90.
11. NABIL, T.E.-D& DOAA, R.M. (2020). Hall Current and Joule Heating Effects on Peristaltic Flow of a Sisko Fluid with Mild Stenosis through a Porous Medium in a Tapered Artery with Slip and Convective Boundary Conditions. *Sains Malaysiana*, 49 (5), 1175-1190.
12. Ramesh, K. & Devakar, M. (2017). Effect of heat transfer on the peristaltic transport of a MHD second grade fluid through a porous medium in an inclined a symmetric Channel. *Chinese Journal of Physics*, 55(3), 825-844.

JOBS



مجلة العلوم الأساسية
Journal of Basic Science



Print -ISSN 2306-5249

Online-ISSN 2791-3279

العدد الرابع عشر

2023م / 1444هـ



مجلة العلوم الأساسية
للعلوم التربوية والنفسية وطرانق التدريس للعلوم الأساسية